Ocean Sci., 10, 177–199, 2014
www.ocean-sci.net/10/177/2014/
doi:10.5194/os-10-177-2014

Ocean Science Open Access

Secchi depth in the Oslofjord–Skagerrak area: theory, experiments and relationships to other quantities

E. Aas[1], **J. Høkedal**[2], **and K. Sørensen**[3]

[1]Department of Geosciences, University of Oslo, Gaustadalleen 21, 0349 Oslo, Norway
[2]Narvik University College, Lodve Langesgt. 2, 8508 Narvik, Norway
[3]Norwegian Institute for Water Research, Gaustadalleen 21, 0349 Oslo, Norway

Correspondence to: E. Aas (eyvind.aas@geo.uio.no)

Received: 9 September 2013 – Published in Ocean Sci. Discuss.: 25 October 2013
Revised: 3 February 2014 – Accepted: 5 February 2014 – Published: 18 March 2014

Abstract. The Secchi depth and its relationships to other properties of the sea water in the Oslofjord–Skagerrak area have been investigated. White and black disks of different sizes have been applied, and the Secchi depth has been observed with the naked eye, through colour filters and with a water telescope. Spectral luminances and illuminances have been calculated from recordings of radiance and irradiance, and attenuation coefficients have been determined. A theoretical expression for the Secchi depth based on luminances has been tested against field observations, and it is found that the field results for the product of Secchi depth and attenuation coefficients are on average only 4 % less than the predicted value for the white disk. For the Secchi depths observed through colour filters or for the black disk, the average field results are more than 30 % smaller than the theoretical estimates. The reduction in the disk diameter from 30 to 10 cm should theoretically reduce the Secchi depths by 13–22 %, while the field observations show an average reduction of 10–20 %. Similarly we find from theory that the removal of sun glitter should increase the Secchi depth by 12 %, while the observed increase is 14 % on average for the white disk. Our overall conclusion is that the theoretical expression works well for the white disk, but less so for the colour filter observations and the black disk.

Statistical relationships between Secchi depths and attenuation coefficients have been determined, and it is found that the root-mean-square errors relative to the mean value are smaller for the beam attenuation coefficients (12–24 %, white disk) than for the vertical attenuation coefficients (16–65 %, white disk). The depth of the 1 % level of surface quanta irradiance (PAR) can be estimated with a relative root-mean-square error of 23 % from observations of the white Secchi depth. Similar estimates of chlorophyll *a* and total suspended material will have rms errors in the range 40–90 %. Our conclusion becomes that the Secchi depth observation is a very useful tool for checking the value and order of magnitude of other related quantities in the Oslofjord–Skagerrak area.

1 Introduction

1.1 Motivation for the present study

The threshold depth of observation for the Secchi disk is a direct measure of the vertical visibility in water, and it is one of several parameters used by environmental authorities to describe water quality. In some branches of aquatic science it is termed transparency. The depth is determined by the optical properties of the water and can therefore be related to these properties. Observations of the Secchi depth can never be satisfactory substitutes for direct recordings of the other optical properties, but they can serve as independent checks of these properties.

The Norwegian Institute for Water Research and the University of Oslo have collected numerous observations of the Secchi depth as well as recordings of other optical quantities. We have analysed parts of this database to check a theoretical expression for the Secchi depth, and we have checked some of the assumptions on which the Secchi depth theory is based, as well as some results that can be deduced from the theory. Different disks and a water telescope have

been applied, and threshold depths have been determined by the naked eye as well as with coloured glass filters in front of the eye. The results are based on observations from the Oslofjord–Skagerrak area. The test of the theoretical expression, as well as the statistical relationships found between Secchi depth and other optical properties, has been the main motivation for this study.

In Sect. 2 we present what is essentially Tyler's (1968) theory of the Secchi depth, and Sect. 3 describes some of the regional environmental characteristics and the applied data sets and instruments. Section 4 estimates the different optical properties appearing in the theoretical expression for the Secchi depth, and the expression as well as an assumption about the applied attenuation coefficients are compared to observations. Empirical relationships between the Secchi depth and other optical properties are discussed in Sect. 5. The results are summed up in Sect. 6.

1.2 History

The visibility of the Pacific Ocean was studied by the Russian naval officer Otto von Kotzebue as early as 1817 by means of a red piece of cloth being lowered into the sea, and on one occasion by a white plate, according to Krümmel (1886). This is probably the first known scientific investigation of the optical properties of the ocean. Other early transparency measurements and occasional observations are mentioned by Boguslawski (1884), a later work by Krümmel (1907), and by Wernand (2010).

In 1866, almost fifty years after von Kotzebue's measurements, Alessandro Cialdi, Commander of the Papal Navy, published a report containing a section by Frater Pietro Angelo Secchi, where the factors influencing the visibility in the sea of submerged disks of different sizes and colourings were discussed (Secchi, 1866). In the years to come the white version of this device became a standard instrument in marine investigations. In some scientific communities the disk is referred to as "the white disk", and in others as "the Secchi disk", although the suggestion of using a white disk came from Cialdi.

Today the marine standard method of measurement is to lower a white disk, with a diameter of approximately 30 cm, supported on a cord and with its plane horizontal, from the ship rail and into the sea to a depth where the disk cannot be seen any longer. The disk is then hauled upwards to a depth where it can be recognised once again. The mean value of the two threshold depths is termed "the Secchi depth". In limnology some communities prefer using a 20 cm disk, painted in black and white quarters, but this device will not be discussed in this paper.

However, during the first century of Secchi depth measurements a satisfactory theory describing the relationship between the threshold depth and the optical properties of the sea was missing. The factors influencing the depth were known (Krümmel, 1889), and Sauberer and Ruttner (1941) had set up the equations governing the contrast and the upward directed light, but the final step connecting the Secchi depth and the attenuation coefficients was not taken. According to Shifrin (1988) Gershun had solved the problem in 1940, but his results were published in Russian and therefore not well known outside the Soviet Union. In the western world the breakthrough came when Tyler (1968) applied a contrast formula, presented sixteen years earlier by Duntley (1952), to derive an expression for the Secchi depth. Holmes (1970) tested the constant of this expression by field measurements. A different contrast formula, including the halo of scattered light around the disk, was suggested by Levin (1980). Preisendorfer (1986) discussed the assumptions and limitations of the Secchi depth theory and procedure, using attenuation coefficients of photopic quantities.

Krümmel (1889) referred to observations made by Austrian oceanographers in the Adriatic and Ionian seas in 1880 with disks of different metals and paintings. Lisitzin (1938) observed the Secchi disk through coloured glass filters in the Baltic Sea as early as in the 1920s, and Takenouti (1950) performed similar measurements in Japanese lakes. Højerslev (1977, 1978) succeeded in relating such glass filter observations to other marine-optical properties. Levin (1980) mentioned recordings with glass filters in the Black Sea. An interesting study of the black disk was made in 1988 by Davies-Colley. Haltrin (1998) reported observations with disks that were painted blue, green and red.

For more than two decades remote sensing of water colour has been used to estimate the Secchi depth (http://www.globcolour.info/data_access_demo.html), which is one of the ESA GlobColour products.

2 Theory of the Secchi depth

An important factor that enters the theory of the Secchi depth is the properties of the human eye as a contrast sensor. Studies in air (Blackwell, 1946) have demonstrated that the human eye is able to distinguish a target from its background down to a lower limit or threshold value of the contrast between the target and its background. In our case the target is the Secchi disk, and the definition of the contrast C becomes $C = (L_D - L)/L$, where L_D is the luminance from the disk and L the luminance from the background. The eye integrates the total spectrum of radiances within the direction to the disk and the background, and weights these radiances by the eye's spectral sensitivity. During daylight conditions this is represented by the photopic sensitivity of the eye, and we have expressed it by the CIE 1924 curve for luminous efficiency (e.g. Walsh, 1958). This curve, which is also termed the photopic luminosity function, has its maximum at 555 nm, half-peak values at 510 and 610 nm, and 1 % of the maximum at 438 and 687 nm. The resulting integrals become the luminances L_D and L. If the eye of the observer is at the depth $z = 0$, which in this paper will mean just beneath the surface, or if

a water telescope is being used, that is a tube through the water surface with a glass window at the bottom, then the observed contrast $C(0)$ at this depth between the nadir luminances $L_D(0)$ and $L(0)$ from the white Secchi disk and the background, respectively, will be

$$C_0 = \frac{L_D(0) - L(0)}{L(0)}. \quad (1)$$

When the Secchi disk is lowered, $L(0)$ remains constant while $L_D(0)$ is reduced until the disk reaches the depth where it disappears from sight, namely the Secchi depth. Then $C(0)$ has been reduced to the threshold value C_t. According to Blackwell (1946) C_t is not a constant, but depends on the angle α subtended by the observed target, the luminance $L(0)$ of the background, the probability of detection and the exposure time. C_t decreases with decreasing detection probability and with increasing α, $L(0)$ and exposure time.

Photometric luminance is not a practical quantity if we want to use the *equation of radiative energy transfer*, because the luminance represents a spectral integral, and therefore its attenuation coefficients are not constant in space, even in optically homogeneous waters. However, when we determine the Secchi depth, we notice that the colour of the disk is the same as that of the surrounding waters. This colour corresponds to the wavelength region where the water has its maximum beam transmittance, which is also where the upward scattered radiance obtains its spectral maximum. We can therefore assume as a first approximation that the observed luminances in Eq. (1) correspond to the radiances at the wavelength of the spectral transmittance maximum. In the present discussion we have let the symbol L represent these monochromatic radiances as well as the spectrally narrow-banded photopic luminances. The magnitude of the errors introduced by the monochromatic assumption will be discussed in Sect. 4.8.

The equation of radiative energy transfer for the nadir radiance L_D from the Secchi disk sounds

$$-\frac{dL_D(z)}{dz} \approx -c\,L_D(z) + L_{*D}(z), \quad (2)$$

where z is the vertical coordinate with zero at the surface and positive downwards, c is the beam attenuation coefficient at the wavelength of maximum transmittance, and L_{*D} is the path function along the path from the disk to the observer.

The same equation for the nadir radiance L from the background becomes

$$-\frac{dL(z)}{dz} \approx -cL(z) + L_*(z). \quad (3)$$

Here L_* is the path function along an upward directed path outside the disk.

Tyler (1968) applied Duntley's (1952) contrast formula and assumed that at each depth z the path function $L_{*D}(z)$ above the Secchi disk is practically uninfluenced by the disk, and therefore approximately equal to the path function $L_*(z)$ of the background. This assumption may be questioned, and especially at positions close to the disk. However, let us assume that it is still valid for most of the path between the disk and the surface. By making the approximation $L_{*D}(z) \approx L_*(z)$ and subtracting Eq. (3) from Eq. (2) we obtain

$$\frac{d[L_D(z) - L(z)]}{dz} \approx c[L_D(z) - L(z)]. \quad (4)$$

Provided c is constant with depth the integration of this equation between the surface and the Secchi depth $z = Z_D$ results in

$$[L_D(0) - L(0)] = [L_D(Z_D) - L(Z_D)]\, e^{-cZ_D}. \quad (5)$$

We recognise the left side of this equation as the numerator of Eq. (1). On the right-hand side we have the radiance $L_D(Z_D)$ which is the reflected part of the downward irradiance $E_d(Z_D)$ incident at the disk. The reflectance of this radiance may be termed ρ_{DL}, defined by

$$\rho_{DL} = \frac{L_D(Z_D)}{E_d(Z_D)}. \quad (6)$$

At the same level outside the disk the upward radiance $L(Z_D)$ will be related to the downward irradiance by the radiance reflectance R_L:

$$R_L(Z_D) = \frac{L(Z_D)}{E_d(Z_D)}. \quad (7)$$

In Eqs. (6)–(7) it is assumed that the downward irradiance at the Secchi depth is practically unaffected by the presence of the disk, and has the same value above as outside the disk. By using Eqs. (6)–(7) the radiances on the right side of Eq. (5) may be written as functions of $E_d(Z_D)$, and Eq. (5) becomes

$$[L_D(0) - L(0)] = [\rho_{DL} E_d(Z_D) - R_L(Z_D) E_d(Z_D)] e^{-cZ_D}. \quad (8)$$

At this point we see that it would be very convenient if we could also express the denominator $L(0)$ on the right-hand side of Eq. (1) as a function of $E_d(Z_D)$. $L(0)$ can be transformed in several ways, but the simplest expression is obtained by using $E_d(z)$ and $R_L(z)$ and writing $L(z)$ as an exponential function of z:

$$L(0) = L(Z_D) e^{K_L Z_D} = R_L(Z_D) E_d(Z_D) e^{K_L Z_D}, \quad (9)$$

where K_L is the average vertical attenuation coefficient of $L(z)$ in the depth range 0–Z_D.

If we insert for the numerator in Eq. (1) from Eq. (8) and for the denominator from Eq. (9), we obtain:

$$C(0) = \frac{L_D(0) - L(0)}{L(0)} = \frac{[\rho_{DL} - R_L(Z_D)] e^{-cZ_D}}{R_L(Z_D) e^{K_L Z_D}} = \frac{[\rho_{DL} - R_L(Z_D)]}{R_L(Z_D)} e^{-(c+K_L)Z_D}, \quad (10)$$

which can be more conveniently written as

$$Z_{\mathrm{D}}(c+K_L)=\ln\left(\frac{\frac{\rho_{\mathrm{DL}}}{R_L(Z_{\mathrm{D}})}-1}{C(0)}\right). \tag{11}$$

The contrast $C(0)$ is equal to the threshold value C_{t}, provided the eye of the observer is below the surface. Tyler (1968) presented a version of Eq. (11), and Hou et al. (2007) obtained a similar expression by using modulation transfer theory.

If the observer's eye is above the surface, the radiance from the direction of the disk will consist of two terms. The first is $L_{\mathrm{D}}(0)\ \tau/n^2$, where τ is the radiance transmittance for a ray of normal incidence at the water–air interface, and n is the index of refraction for water. This is the transmitted part of the radiance $L_{\mathrm{D}}(0)$. The other term is the radiance L_{r} from sun and sky reflected at the surface towards the observer. The sum of the terms becomes $L_{\mathrm{D}}(0)\ \tau/n^2+L_{\mathrm{r}}$. Similarly the radiance from the background will now be $L(0)\ \tau/n^2+L_{\mathrm{r}}$. It should be noted that the first part of the latter sum is the quantity that is usually termed the water-leaving radiance L_{w}

$$L_{\mathrm{w}}=L(0)\frac{\tau}{n^2}. \tag{12}$$

The contrast of the Secchi disk observed in air through a flat sea surface becomes

$$\begin{aligned}C_{\mathrm{air}}&=\frac{\left(L_{\mathrm{D}}(0)\frac{\tau}{n^2}+L_{\mathrm{r}}\right)-\left(L(0)\frac{\tau}{n^2}+L_{\mathrm{r}}\right)}{\left(L(0)\frac{\tau}{n^2}+L_{\mathrm{r}}\right)}\\&=\frac{L_{\mathrm{D}}(0)-L(0)}{L(0)\left(1+\frac{L_{\mathrm{r}}}{L_{\mathrm{w}}}\right)}=\frac{C(0)}{1+\frac{L_{\mathrm{r}}}{L_{\mathrm{w}}}}.\end{aligned} \tag{13}$$

If capillary waves are present, they will have a blurring effect on the image of the disk, and as a result the apparent contrast will be reduced. Preisendorfer (1986) expressed the transmittance W of $C(0)$ at the water–air interface as a function of the angular subtense of the Secchi disk as seen from just below the surface, and the variance of the slopes of the capillary waves. In our notation his expression can be written

$$W=1-\exp\left(-\frac{D^2k}{Z_{\mathrm{D}}^2U}\right)\le 1, \tag{14}$$

where the symbols k and U represent the constant 787 m s^{-1} and the wind speed, respectively, and D is the diameter of the disk. When W is included in Eq. (13), the equation becomes

$$C_{\mathrm{air}}=\frac{C(0)}{1+\frac{L_{\mathrm{r}}}{L_{\mathrm{w}}}}W=C_{\mathrm{t}}. \tag{15}$$

In this case it is C_{air} that represents the threshold value C_{t}. Equation (15) can also be written as

$$C(0)=\frac{C_{\mathrm{t}}}{W}\left(1+\frac{L_{\mathrm{r}}}{L_{\mathrm{w}}}\right). \tag{16}$$

The contrast $C(0)$ has to be greater than C_{t}, and in inverse proportion to the blurring effect W. $C(0)$ will also be a linear function of the ratio $L_{\mathrm{r}}/L_{\mathrm{w}}$ between the reflected and water-leaving radiances. The greater the surface reflection is, the greater $C(0)$ has to be. It will be convenient for our purposes to express L_{r} and L_{w} as functions of the same input above the surface, namely the downward irradiance E_{air}. L_{r} can be written as

$$L_{\mathrm{r}}=\bar{\rho}_{L,\mathrm{air}}E_{\mathrm{air}}, \tag{17}$$

where $\bar{\rho}_{L,\mathrm{air}}=L_{\mathrm{r}}/E_{\mathrm{air}}$ is the Fresnel-reflected radiance towards the zenith, depending on the slope distribution of the surface and the angular distribution of radiance from sky and sun. L_{w} can be transformed by using the quantity $\mathfrak{R}$ introduced by Morel and Gentili (1996):

$$\mathfrak{R}=\frac{L_{\mathrm{w}}}{L(0)}\frac{E_{\mathrm{d}}(0)}{E_{\mathrm{air}}}=\frac{L_{\mathrm{w}}}{E_{\mathrm{air}}}\frac{1}{R_L(0)}. \tag{18}$$

By inserting for L_{r} and L_{w} from Eqs. (17) and (18) into Eq. (16) we obtain

$$C(0)=\frac{C_{\mathrm{t}}}{W}\left(1+\frac{L_{\mathrm{r}}}{L_{\mathrm{w}}}\right)=\frac{C_{\mathrm{t}}}{W}\left(1+\frac{\bar{\rho}_{L,\mathrm{air}}}{\mathfrak{R}R_L(0)}\right). \tag{19}$$

Equation (11) can then be written, by substituting for $C(0)$ from Eq. (19), as

$$Z_{\mathrm{D}}(c+K_L)=\ln\left(\frac{\frac{\rho_{\mathrm{DL}}}{R_L(Z_{\mathrm{D}})}-1}{1+\frac{\bar{\rho}_{L,\mathrm{air}}}{\mathfrak{R}R_L(0)}}\frac{W}{C_{\mathrm{t}}}\right)=\ln(A), \tag{20}$$

where A is defined as the product of the two fractions inside the greater parentheses. This is our basic equation for the threshold depth of the white Secchi disk observed from above the surface. The numerator of the first fraction is a function of the reflective properties ρ_{DL} of the disk and the radiance reflectance $R_L(Z_{\mathrm{D}})$ of the background at the Secchi depth, the denominator is a function of the ratio between the surface-reflected and water-leaving radiances, W represents the influence of capillary waves on the transmittance of $C(0)$ through the surface, while C_{t} is the threshold contrast of the human eye.

Observation of the disk through coloured glass filters will change the threshold depths, and the coefficients c, K_L, ρ_{DL}, R_L, $\bar{\rho}_{L,\mathrm{air}}$ and $\mathfrak{R}$ will refer to other wavelengths than the spectral region of maximum transmittance. Otherwise Eq. (20) remains the same.

Equation (20) contains 10 variables, and if we had had precise values of these at a large number of stations, it would have been very interesting to test the equation. However, the usefulness of an expression needing the input of nine variables to predict the one remaining would be limited. It would have been far more convenient if the right-hand side of Eq. (20) had been a constant. The Secchi depth Z_{D} would then become linearly proportional to $1/(c+K_L)$, or $(c+K_L)$

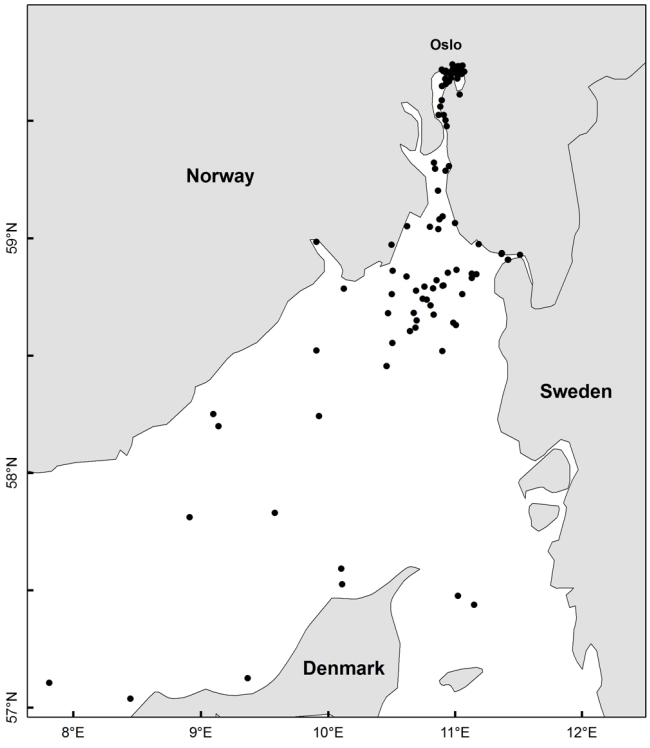

Fig. 1. Locations of the stations.

would be proportional to $1/Z_D$. Unfortunately, R_L, $\bar{\rho}_{L,\mathrm{air}}$ and $\Re$ are variables determined by the optical properties of the sea water and sea surface, C_t is a function of the Secchi depth and the background luminance, while W varies with the wind speed and the Secchi depth. Thus the variables on the right-hand side of Eq. (20) are neither independent nor constant, but the logarithmic function will reduce the variation of the expression inside the parentheses, which is why the equation may still provide a useful support for other marine-optical observations.

A more practical form of Eq. (20) for our purposes is

$$Z_D(c+K_L) = \ln\left(\frac{\rho_{DL}}{R_L(Z_D)} - 1\right) - \ln\left(1 + \frac{\bar{\rho}_{L,\mathrm{air}}}{\Re R_L(0)}\right) + \ln(W) - \ln(C_t) = \ln(A_1) - \ln(A_2) + \ln(W) - \ln(C_t) = \ln(A), \quad (21)$$

where A_1 and A_2 are defined by the expressions inside the parentheses. In order to test Eq. (21) we will calculate the mean value of the expression on the left-hand side of the equation, as well as the mean values of the different logarithmic functions on the right-hand side.

Some special cases can be pointed out:

- For a perfectly black disk, that is a disk where $\rho_{DL} = 0$ (Eq. 6), the quantity A_1 of Eq. (21) obtains the value -1, while C_t will be a negative number. The two negative signs will cancel each other inside the parenthesis of $\ln(A)$.
- If $L_r/L_w \approx 0$ (Eqs. 16–17), the quantity A_2 becomes 1 and $\ln(A_2) = 0$.
- When Z_D is observed by using a water telescope, the effects of waves and surface-reflected sky radiance are eliminated, so that $W = 1$ in addition to $\bar{\rho}_{L,\mathrm{air}} \approx 0$, and $\ln(A_2) = \ln(W) = 0$.

The different steps leading up to Eq. (21) make it possible to discuss the different factors that influence the Secchi depth. We will determine the attenuation coefficients c and K_L from calculated luminances in Sect. 4.1, estimate mean values of the quantities $\ln(A_1)$, $\ln(A_2)$, $\ln(W)$ and $\ln(C_t)$ in Sects. 4.2–4.3, and then see how the mean value of $(c+K_L)_{\mathrm{phot}} Z_{D,\mathrm{white}}$ relates to the combined effects of these quantities according to Eq. (21) in Sect. 4.4. In Sects. 4.5–4.7 we will look at the effects of colour filters, disk size, sun glitter, ship shadow and waves. Section 4.8 will check how the assumption made early in Sect. 2, about attenuation coefficients of luminances in photopic units corresponding to monochromatic coefficients at the wavelength of maximum transmittance, agrees with our results.

3 Environment, data sets and methods

In this section we describe briefly the environmental conditions of the investigated area, the data sets and the applied instruments and methods.

3.1 Environmental conditions

Our main area of investigation has been the Oslofjord, with additional data from the Skagerrak and two stations from the Kattegat (Fig. 1). The waters of the Oslofjord are in general eutrophic due to a supply of nutrients from the surrounding settlements (Ibrekk and Holtan, 1988). There is an estuarine circulation in the fjord, but rather weak in the inner part of the fjord. There is usually an upper and a lower layer separated by a transition layer, the pycnocline. The surface layer may sometimes be well-mixed, but often there will be a gradual change of properties from the upper 1–2 m down to the pycnocline (Aure et al., 1996; Staalstrøm et al., 2012). Salinities in the surface layer are typically in the range 20–29, and in deep waters up to 34 (Gade, 1963, 1967; Staalstrøm et al., 2012). Such values are of interest because a low salinity means a high content of fresh water, and this may indicate a high content of yellow substance, which is a significant optical component in these areas. The Secchi depth is found above the lower layer in the fjord. Maps of the Secchi depth, observed in 1988, have been presented by Aas et al. (1989), and Andresen (1993) has studied seasonal and annual changes of the Secchi depth in the period from 1936 to 1992.

The Skagerrak serves as a transition zone between the North Sea and the Baltic (Aarup et al., 1996a, b; Højerslev et al., 1996), and it also supplies the more saline waters to the Oslofjord. A very thorough analysis of the Secchi depths in the North Sea–Baltic Sea region has been made by Aarup (2002). Surface salinities in the northeastern part of the Skagerrak are in the range 25–32, and below the surface layer the waters become more Atlantic, with salinities up to 35 (Højerslev et al., 1996; Aarup et al. 1996a).

The environmental parameters salinity, wind speed, cloudiness and Secchi depth are presented for the different parts of our investigated area in Table 1. The salinity ranges are based on observations from different years. The Secchi data for the Inner and Outer Fjord are based on observations from 1982–1992, tabulated by Andresen (1993), while the data for the Skagerrak are observations from 1900–1999, based on a figure presented by Aarup (2002). The Norwegian Meteorological Institute has calculated mean values and standard deviations of wind speed and cloudiness at two locations: Fornebu, representing the Inner Fjord, and the Færder Lighthouse at 59.03° N, representing the border between the Outer Fjord and the Skagerrak. The input data are diurnal means from the entire 30 yr period 1961–1990. It should be pointed out, however, that cloudiness in these regions does not follow a Gaussian distribution.

Average values for the inherent optical properties of the Skagerrak–Outer Oslofjord area were found by Sørensen et al. (2007). At 442 nm the absorption coefficient of yellow substance was $a_y(442) = 0.62\,\mathrm{m}^{-1}$, the bleached particle absorption $a_{bp}(442) = 0.065\,\mathrm{m}^{-1}$, and the particle scattering $b_p(442) = 0.645\,\mathrm{m}^{-1}$. The approximate spectral variations of these coefficients within the range 400–550 nm were $a_y(\lambda) = a_y(442)\,e^{-(0.0105\,\mathrm{nm}^{-1})(\lambda - 442\,\mathrm{nm})}$, $a_{bp}(\lambda) = a_{bp}(442)\,e^{-(0.0089\,\mathrm{nm}^{-1})(\lambda - 442\,\mathrm{nm})}$ and $b_p(\lambda) = b_p(442)\left[\frac{442\,\mathrm{nm}}{\lambda}\right]^{0.376}$ where λ is the wavelength, implying that the contributions from yellow substance and particles to the attenuation coefficient c are of the same order of magnitude in the blue part of the spectrum, while particles will tend to dominate in the red part.

During 2002–2003 spectra of upward radiance just beneath the surface in the Oslofjord and Skagerrak were recorded for calibration and validation purposes (Sørensen et al., 2003, 2004, 2007), related to the ESA committee MAVT. The peak values of the upward radiance spectra usually occurred in a wavelength range from 480 to 570 nm, with the mean wavelength around 525 nm. The bluish maxima were only observed at stations that were strongly influenced by Atlantic waters (salinity close to 35). The half-peak bandwidths of these spectra were typically 150 nm. Figure 2 shows the mean value of the spectra at the MERIS channels, normalised at 555 nm, as well as the standard deviation. An example of the rather rare Atlantic spectrum is included for comparison. When the radiance spectra are multiplied by the CIE photopic efficiency function described in Sect. 2, the shapes of the resulting spectral upward luminances are significantly narrowed. The half-peak bandwidths will now be typically around 80 nm, and the peak values will be situated between 550 and 570 nm.

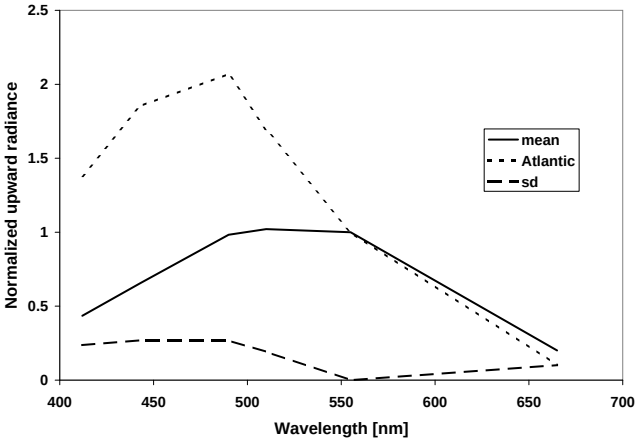

Fig. 2. Mean value of the upward radiance spectra just beneath the surface, normalised at 555 nm and based on 48 stations, and the standard deviation of the normalised spectra. For comparison a station of typical Atlantic water is presented.

3.2 First data set and methods

The first data set consists of data from 26 stations, collected in 1992 between May and December, in the Inner Oslofjord. The set contains the threshold depths of different types of Secchi disks observed by the open eye as well as with coloured glass filters. Two sizes of white and black disks were used, the standard size with a diameter of 30 cm, and a smaller one with a diameter of 10 cm. It is difficult to obtain a perfectly black disk, defined as a disk with no reflectance at all. Disks painted black or made from black materials may still have a radiance reflectance ρ_{DL} that is greater than the corresponding reflectance R_L of the background water. The closest approximation to the non-reflecting disk that we have used has been a bowl-shaped lamp shade of brass, painted black for the scientific purpose, with diameter 30 cm. This device was originally acquired by the University of Copenhagen, but later on kindly donated to the University of Oslo by N. K. Højerslev. The instrument is supposed to work in principle very much like the light trap termed Rayleigh's Horn. Measurements were also taken with a 3.0 m-long water telescope (donated by the University of Copenhagen) that reached from the ship rail into the sea. The properties of the photopic sensitivity of the eye alone and in combination with blue, green and red glass filters (Mikaelsen and Aas, 1990) are shown in Table 2. The filters were produced by Schott and termed BG12, VG9 and RG1. The latter filter corresponds to OG590 in the latest Schott catalogue. The combined effect of

Table 1. Environmental conditions in the Oslofjord–Skagerrak area. S is salinity range between the surface and the Secchi depth, U is mean ± standard deviation of wind speed in m s^{-1}, C is mean ± sd of cloudiness in octas, and $Z_{D,white}$ is mean ± sd of Secchi depth in m.

Area	Inner Fjord north of 59.67° N	Outer Fjord 59.00°–59.67° N	Skagerrak 57.00°–59.00° N
S (all year)[a,b]	15–28	16–30	20–32
U (summer)[c]	2.8 ± 0.5	6.7 ± 1.1	
U (winter)[c]	2.0 ± 0.7	7.9 ± 1.6	
C (summer)[c]	5.0 ± 0.8	4.8 ± 0.7	
C (winter)[c]	5.5 ± 0.9	5.6 ± 0.9	
$Z_{D,white}$ (summer)[d]	4.4 ± 1.7	4.3 ± 1.8	
$Z_{D,white}$ (winter)[d]	10.5 ± 2.8	11.1 ± 3.2	
$Z_{D,white}$ (all year)[d,e]	7.4 ± 2.3	7.7 ± 2.6	8.3 ± 2.8

References: [a] Gade (1963, 1967); Aure et al. (1996); Staalstrøm et al. (2012); [b] Aarup et al. (1996a); Højerslev et al. (1996); [c] Norwegian Meteorological Institute (personal communication, 2014); [d] Andresen (1993); [e] Aarup (2002).

eye sensitivity, filter transmittance and a typical spectrum of upward luminances $L(0)$ is also shown, and we see that the half-peak bandwidth of the naked eye is reduced from 100 to 78 nm, otherwise the bandwidths and peak wavelengths remain the same. The Secchi depth was observed on both the sunlit and shaded sides of the ship.

The radiance reflectance ρ_{DL} of the white disk was determined in 1992 from laboratory recordings of the spectral downward irradiance E_d and the corresponding reflected upward radiance L_D from the white disk, as expressed by Eq. (6). Both were measured in water just above the submerged disk. In order to avoid the shadow of the radiance meter on the disk, the instrument could not be held directly above it, but at an angle of 30°–40° away from the axis of the disk. Still, we think that the obtained values of ρ_{DL} were close to the correct ones, being 0.25–0.29–0.30 at the wavelengths 450–520–550 nm, respectively. These values will be discussed in Sect. 4.2.

The accuracy of a Secchi depth observation depends mainly on the wind conditions. Winds will produce waves and may make the ship drift, with a sloping line from the observer down to the disk as a result. It will then become more difficult for the observer to estimate the correct depth below the waves. Other effects of waves are discussed in Sects. 4.2 and 4.3, and values of observed wind speed are presented for the different investigated areas in Table 1. Based on experience we estimate the possible error of $Z_{D,white}$ to be in the range 0.2–0.5 m, depending on wind speed. It may be mentioned that the observations in this and the other data sets were made by experienced oceanographers.

In addition to the Secchi observations quanta irradiance was recorded in the sea with the Underwater Quantum Sensor LI-192SB from LI-Cor, inc., Lincoln, Nebraska, and with the LI-190SB Quantum Sensor on deck as a reference.

3.3 Second data set and methods

A second data set consists of 143 stations from the Inner and Outer Oslofjord, collected between 1973 and 2008 by the University of Oslo during courses and project excursions, with recordings of quanta irradiance and Secchi depths. The period of observation included all months from February to December. The Secchi depth was determined with the 30 cm white disk on the sunlit side of the ship, and quanta irradiance was recorded with the Li-Cor instrument mentioned above.

3.4 Third data set and methods

The third data set consists of observations at 79 stations. Secchi depths, spectral irradiances, radiances, and absorption and attenuation coefficients were measured in the Oslofjord–Skagerrak area during the years 2002–2003, in the summer period from early May to early September.

The Secchi depth was observed with the 30 cm white disk, by the naked eye and with colour filters, often on both the sunlit and shaded sides of the ship. Vertical sub-surface profiles of the downward and upward irradiances and the upward radiance were measured with the PRR-600 from Biospherical Instruments, San Diego, California, with the deck instrument PRR-610 used as a reference. The spectral channels were 412, 443, 490, 510, 555 and 665 nm, corresponding to the channels of the satellite sensors SeaWiFS and MERIS. Vertical profiles of the upward radiance L and the downward and upward irradiances E_d and E_u were recorded. According to the radiance model of Aas and Højerslev (1999), the quantity $Q = L/E_u$ should obtain values in the interval from π to 2π only, and a few stations where Q lay outside this range have been omitted. Immersion coefficients determined by the manufacturer and self-shading effects (Gordon and Ding, 1992; Zibordi and Ferrari, 1995; Aas and Korsbø, 1997) were taken into account. Radiances and irradiances were plotted in semi-logarithmic diagrams and extrapolated

Table 2. Wavelength λ_p of peak value and half-peak bandwidth $\Delta\lambda$ of the eye's photopic sensitivity, alone and in combination with the upward spectral luminance L_u; for the open eye and with filters for the white disk (Mikaelsen and Aas, 1990).

	Open (white and black disk)	Blue filter	Green filter	Red filter
Eye's sensitivity				
λ_p [nm]	555	460	540	620
$\Delta\lambda$ [nm]	100	48	56	38
Eye's sensitivity and L_u				
λ_p [nm]	555	470	540	620
$\Delta\lambda$ [nm]	78	47	55	34

up to the surface. The uncertainty of the resulting surface values was estimated to be ±10 %. A few series of spectral upward radiance just beneath the surface, recorded with the hyperspectral Ramses-ARC radiance sensor from TriOS, have been included to examine the wavelength of the spectral peak.

Vertical profiles of the spectral absorption and scattering coefficients were recorded with an ac-9 from WET Labs, Philomath, Oregon. The applied instrument records at 412, 440, 488, 510, 532, 555, 650, 676, and 715 nm. The data were cleaned for obvious noise, and unrealistic spikes were avoided by using a median filter, resulting in an estimated uncertainty of ±10 %. The recordings with the Biospherical instrument and the ac-9 were analysed and sent to the ESA for calibration and validation purposes (Sørensen et al., 2003, 2004, 2007).

At 19 stations from the 2002–2003 data set chlorophyll *a* (Chl) and total suspended material (TSM) were sampled on glass fibre filters. The concentrations of Chl were determined by the high-performance liquid chromatographic (HPLC) method, and the TSM by a gravimetric method (Sørensen et al., 2007, and references therein).

Figure 1 shows the locations of the stations for the three data sets. The Inner Fjord contains data from all three sets (168 stations), the Outer Fjord data from the second and third sets (48 stations), while the Skagerrak only contains data from the third set (32 stations).

Tables 3, 5, 6, 7, and 9 are based on data solely from the third set, Table 4 on data from the first and third sets, while Table 8 has applied data from all three sets.

4 Test of Eq. (21) in photopic units

In Sects. 4.1–4.3 we will obtain mean values for the different terms in Eq. (21), and in Sect. 4.4 we will test the equation with these values. Other results of our Secchi depth experiments, related to Eq. (21), will be discussed in Sects. 4.5–4.8.

4.1 Values of c_{phot} and $K_{L,\text{phot}}$

In Sect. 2 it was pointed out that the luminance is not a practical quantity in our marine-optical research, because the corresponding coefficient of beam attenuation will depend on the spectral shape of the luminance at the point where the attenuation starts and the distance along the beam. The coefficient c of Eq. (4) describes the beam attenuation of two different luminances: (1) the upward luminance from the disk and (2) the corresponding upward luminance from the surrounding waters. The radiance reflectance ρ_{DL} of the white Secchi disk is defined by Eq. (6). If the albedo of the disk had been 1 and the disk had acted like a perfect Lambert diffuser, the reflected radiance would have been constant for all directions with a radiance reflectance equal to $1/\pi = 0.32$. A real non-perfect Secchi disk will not have this value, but a number of the same order of magnitude. Tyler (1968) applied an estimate of ρ_{DL} equal to $0.82/\pi = 0.26$. Haltrin (1998) presented albedos for white and coloured disks, and provided the disks had acted like perfect diffusers, the values of $\rho_{\text{DL}}$for the white disk would have been 0.23–0.26–0.26 at 450–520–550 nm. Our earlier determinations of ρ_{DL}, described in Sect. 3.2, are very close to the values presented above, being 0.25–0.29–0.30 at the wavelengths 450–520–550 nm, respectively. The latter values have been applied here.

From the recorded spectral downward irradiances $E_d(Z_D)$ at the Secchi depth in the Oslofjord and Skagerrak the reflected upward radiances $L_D(Z_D)$ from the disk were then estimated by Eq. (6). The beam attenuations of the spectral radiances from this depth and up to the surface were calculated by applying recorded values of spectral c, and the resulting spectrum of radiances just beneath the surface was determined. The radiance spectra at the Secchi depth and at the surface were then integrated spectrally by using the photopic efficiency function, and from the resulting two luminances the efficient attenuation coefficient $c_{\text{phot,disk}}$ could be obtained. The attenuation coefficient c_{phot} of the upward background luminance $L(z)$ between the Secchi depth and the surface was calculated in a similar way. All values of the ratio $c_{\text{phot,disk}}/c_{\text{phot}}$ have been found to lie within the range 1.00 ± 0.01. Thus the two attenuation coefficients are practically equal.

The upward luminances at the surface and the Secchi depth, $L(0)$ and $L(Z_D)$, were found by integrating the spectral upward luminances at the two depths, and then $K_{L,\mathrm{phot}}$ could be determined by using Eq. (9). Because the observed values of Z_D for the black disk were less than for the white disk (Table 3), the spectral luminance $L(Z_D)$ at this smaller depth differed from the former luminance, and accordingly c_{phot} and $K_{L,\mathrm{phot}}$ for the black disk also became slightly different (Table 3). The attenuation coefficients c_{phot} and $K_{L,\mathrm{phot}}$ for the luminances observed through colour filters were calculated in the same way as for the open-eye coefficients.

4.2 Values of ρ_{DL}, R_L, $\Re$, $\bar{\rho}_{L,\mathrm{air}}$, $\ln(A_1)$ and $\ln(A_2)$

It was explained in Sect. 4.1 how the downward illuminance and the reflected luminance from the disk were determined, and which spectral values of ρ_{DL} we have applied. From the latter values ρ_{DL} was estimated equal to 0.30 for the white disk observed through the red filter, and by definition equal to 0 for the black disk. The values of ρ_{DL} for the white disk observed with the open eye and through the blue and green filters were determined by using the spectral recordings of downward illuminance, and the results are 0.29, 0.27 and 0.29, respectively (Table 3).

The mean value of $R_L(0)$, defined as the ratio between upward luminance and downward illuminance just beneath the surface (Eq. 7), has been calculated from 32 stations as 0.56 % for the open eye. This value is valid for both the white and black disks (Table 3). However, the mean value of $R_L(Z_D)$ at the Secchi depth becomes different for the white and black disks, being 0.83 % and 0.61 %, respectively, and the reason for this is that Z_D differs for these disks. The estimated values of R_L for the colour filters are shown in Table 3.

It was found by Aas et al. (2009) that an average value for the quantity $\Re$ in the Oslofjord–Skagerrak area was 0.506 ± 0.045 for solar altitudes between 15° and 60°, which is close to similar results found by Morel and Gentili (1996) and Mobley (1999). $\Re$ was assumed to be independent of wavelength, and the found value has been applied for both the white and black disks (Table 3).

The radiance reflected towards the zenith at the surface of the sea is described by the radiance reflectance $\bar{\rho}_{L,\mathrm{air}}$. Its value for a clear sky depends on the angular distribution of sky radiance, the solar altitude, the ratio between diffuse sky irradiance and direct solar irradiance, and the statistical distribution of surface slopes. Polynomials for calculating $\bar{\rho}_{L,\mathrm{air}}$ were obtained during a previous work (Aas, 2010). The problem was simplified by looking at average values for all possible angles between wind direction and solar azimuth, using the Cox and Munk model with a one-dimensional Gaussian distribution for the surface slopes (Cox and Munk, 1954a, b). The input was spectral sky and solar radiance data from the Oslo region (Høkedal and Aas, 1998; Aas and Høkedal, 1999). However, there is the problem that while the wave height and wave spectrum are functions of wind speed, duration and fetch, only the wind speed appears in the Cox–Munk model. A comparison between wave heights and wind speeds at those of our stations where both quantities were observed, shows that in many cases either the wind duration or the fetch must have had a limiting effect on the wave height. Still, the mean values ± the standard errors of wind speed and wave height, $5.5 \pm 0.4\,\mathrm{m\,s^{-1}}$ and 0.7 ± 0.1 m, respectively, are consistent with the conditions for a fully developed sea shown in the diagram by Gröen and Dorrestein (1976, also shown by WMO, 1998). Accordingly we have tentatively chosen the wind speed $5.5\,\mathrm{m\,s^{-1}}$ to represent the average conditions. The mean values and standard deviations of $\bar{\rho}_{L,\mathrm{air}}$ shown in Table 3 are based on 10 different cases of atmospheric radiance distribution. The values of $\bar{\rho}_{L,\mathrm{air}}$ for the open eye (the white and black disks) and for the blue, green and red filters were obtained from atmospheric radiance distributions at 550, 470, 540 and 620 nm, respectively (Table 3).

The estimated mean value and standard deviation of $\ln(A_1)$ were obtained by using the value of ρ_{DL} shown in Table 3, and varying values of $R_L(Z_D)$ for each station. Similarly the values of $\ln(A_2)$ were found from the values of $\bar{\rho}_{L,\mathrm{air}}$ and $\Re$ suggested by Table 3 and varying values of $R_L(0)$. The results for $\ln(A_1)$ and $\ln(A_2)$ are presented in Table 3.

The size distributions of the optical quantities estimated here are often highly asymmetric, implying that the standard deviation does not always provide a satisfactory description of the range of variation, like when the standard deviation is greater than the mean value.

4.3 Value of C_t and W

It was mentioned in Sect. 2 that according to Blackwell (1946) the contrast threshold C_t will depend on the angle α subtended by the observed target, the luminance $L(0)$ of the background, the probability of detection, and the exposure time. In Part I of Blackwell's investigation circular targets, brighter than the background, had an exposure time of six seconds, and the contrast thresholds were those that corresponded to a 50 % detection probability. In Part II the targets were darker than the background, and the conclusion was that in most cases negative stimuli are equivalent to positive stimuli of the same area and contrast. The results in Part III were obtained when an indefinitely long exposure time was used. A comparison between Blackwell's experiments and Secchi disk observations is not straightforward, because Blackwell's target images were constant during the time of exposure, while at sea the image of the Secchi disk is usually varying. We have chosen an indefinitely long exposure time and the highest detection probability, 100 %.

The apparent angle α from the observer's eye across the Secchi disk is a function of the diameter D of the disk, the height H of the observer's eye above the surface of the sea, the Secchi depth Z_D and the refractive index n. Because α is a small angle, $\tan(\alpha/2)$ can be approximated by $\alpha/2$, and

Table 3. Mean value and standard deviation of the different quantities and terms of Eqs. (19)–(20) in the Oslofjord and Skagerrak, for the 30 cm white and black disks. Colour filters are for the white disk. Recordings of radiance and irradiance at 32 stations have been applied.

	White	Blue filter	Green filter	Red filter	Black
Z_D [m]	7.8 ± 2.7	4.1 ± 1.4	5.7 ± 2.0	4.2 ± 1.5	2.0 ± 0.7
$(c + K_L)_{\text{phot}}$ [m^{-1}]	1.09 ± 0.67	1.41 ± 0.99	1.08 ± 0.67	1.48 ± 0.56	1.11 ± 0.68
c_{phot} [m^{-1}]	0.83 ± 0.51	0.97 ± 0.65	0.83 ± 0.52	1.03 ± 0.41	0.84 ± 0.51
$K_{L,\text{phot}}$ [m^{-1}]	0.26 ± 0.19	0.44 ± 0.36	0.25 ± 0.18	0.45 ± 0.18	0.27 ± 0.19
ρ_{DL} [%]	29 ± 0	27 ± 1	29 ± 0	30	0
$R_L(0)$ [%]	0.56 ± 0.37	0.47 ± 0.38	0.70 ± 0.47	0.17 ± 0.12	0.56 ± 0.37
$R_L(Z_D)$ [%]	0.83 ± 1.38	0.66 ± 1.33	0.80 ± 1.09	0.28 ± 0.13	0.61 ± 0.51
$\bar{\rho}_{L,\text{air}}$ [%]	0.12 ± 0.08	0.20 ± 0.10	0.14 ± 0.09	0.10 ± 0.08	0.12 ± 0.08
$\Re$ [%]	51	51	51	51	51
C_t [%]	0.56 ± 0.02	0.67 ± 0.12	0.56 ± 0.03	0.59 ± 0.10	-0.54 ± 0.01
W [%]	33 ± 23	66 ± 25	49 ± 27	64 ± 25	94 ± 8
$\ln(A_1)$	3.9 ± 0.7	4.1 ± 0.7	3.8 ± 0.6	4.7 ± 0.4	0
$\ln(A_2)$	0.4 ± 0.1	0.7 ± 0.2	0.4 ± 0.1	0.9 ± 0.3	0.4 ± 0.1
$\ln(W)$	-1.3 ± 0.7	-0.5 ± 0.4	-0.9 ± 0.6	-0.5 ± 0.4	-0.1 ± 0.1
$\ln(C_t)$	-5.2 ± 0.0	-5.0 ± 0.2	-5.2 ± 0.1	-5.1 ± 0.1	-5.2 ± 0.0
$\ln(A)$	7.3 ± 0.9	7.9 ± 0.7	7.8 ± 0.8	8.4 ± 0.7	4.7 ± 0.1
$Z_D(c + K_L)_{\text{phot}}$	7.0 ± 1.3	4.8 ± 1.2	5.1 ± 0.9	5.5 ± 0.7	1.9 ± 0.3

$\tan(j)$, where j is the corresponding angle of refraction in water, can be approximated by $\alpha/(2n)$, using Snell's Law. The angle α in radians becomes

$$\alpha = \frac{D}{H + (Z_D/n)}. \quad (22)$$

If we use Eq. (22) with $D = 0.3$ m, $H = 3$ m, and $n = 1.33$, and if Z_D lies in the interval from 0.5 to 14 m, then the angle α across the Secchi disk will lie between 1.3° and 5.1°. This is within the range in Blackwell's study where the angles of α extended from 0.01° to 6°. Our recordings showed that the background luminances $L(0)$ in the Oslofjord–Skagerrak area were in the range 0.4–1600 cd m^{-2} for the observations with open eye and colour filters. Blackwell's luminances extended from 3×10^{-6} to 3400 cd m^{-2}. Thus our environmental conditions were within the ranges described by Blackwell's experiments. We have selected those of Blackwell's data that are closest to our observed background luminances and angles of subtense, and interpolated these data to fit our ranges. The estimated mean values of C_t and $\ln(C_t)$ for the 30 cm disk, observed with the open eye and through colour filters, are presented in Table 3.

Rather than calculating C_t for each single case and then finding the mean value and standard deviation from the resulting data set, we have found it necessary to restrict the calculations of C_t to the mean, maximum and minimum conditions. The mean conditions were assumed to produce the mean value of C_t, and a crude estimate of the standard deviation was obtained by the expression $(C_{t,\max} - C_{t,\min})/4$. For a normal distribution, 95 % of the observations will fall within a range of ±2 standard deviations from the mean value.

In Table 3 the mean value of C_t is 0.56 % for the white disk, and the mean value of $\ln(C_t)$ becomes −5.2. Krümmel (1889) referred to Helmholtz for the threshold contrast $1/133 = 0.75$ % which produces $\ln(C_t) = -4.9$. The relative difference between the last number and our estimate is only 6 %. Tyler (1968) applied $C_t \approx 0.66$ %, leading to $\ln(C_t) = -5.0$, which is even closer to our estimate. Gordon and Wouters (1978) applied C_t values from 0.15 to 0.6 % or $\ln(C_t)$ from −5.1 to −6.5 in their model studies. Højerslev (1986) deduced from his Baltic recordings a threshold contrast slightly greater than our estimate, $C_t = (0.70 \pm 0.03)$ %, resulting in $\ln(C_t) = -(4.96 \pm 0.04)$. Considering that C_t is not supposed to be a constant, these values are surprisingly similar.

It is noteworthy that Blackwell's experiments involved both the colour and night visions of the human eye. It is well known that night vision requires some time to be activated and adapted, and that a sudden bright glint may temporarily change the vision from night to colour mode. The range where both colour and night visions are active, termed mesopic vision, is 0.001–10 cd m^{-2} according to the CIE. Thus some of our colour filter observations are within this range, but to what extent the varying light conditions have influenced the resulting Secchi depths, we cannot say.

Since our Secchi depths usually are from coastal areas where the surrounding land masses reduce the influence of the wind on the ordinary sea waves, the use of Eq. (14) may perhaps also be overestimating the effect of the wind on the capillary waves. Still, we have tentatively estimated W by using the observed wind speeds and Secchi depths. The average values of W and $\ln(W)$, based on the 32 stations constituting

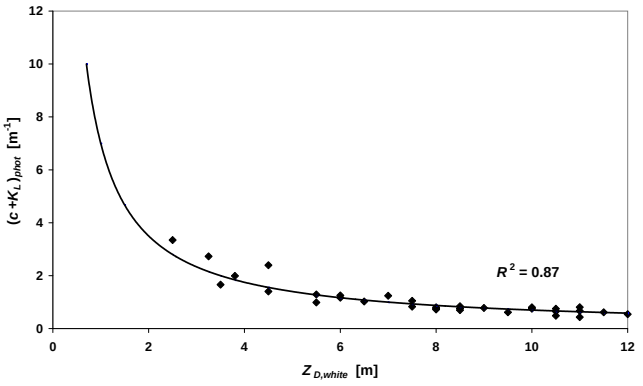

Fig. 3. $(c + K_L)_{\text{phot}}$ as a function of $Z_{\text{D,white}}$. The line is the function $(c + K_L)_{\text{phot}} = 7.0/Z_{\text{D,white}}$. See text in Sect. 4.4 for discussion. R^2 is the coefficient of determination for this line.

the data set where we have complete observations of c, K_L and R_L, are shown in Table 3.

4.4 Value of ln(A) and comparison to observations of $Z_{\text{D,white}}\,(c + K_L)_{\text{phot}}$

There are different ways to test Eq. (21) and to estimate a value for ln(A), and the result will depend on the chosen method. By using the estimated mean values of ln(A_1), ln(A_2), ln(W) and ln(C_t) from Table 3, ln(A) in Eq. (21) obtains the value 7.3 for the 30 cm white disk. The mean value of $Z_{\text{D,white}}(c + K_L)_{\text{phot}}$, found from observations, is 7.0 (Table 3), which is 4 % less than the value predicted by ln(A). Early in the analysis it was discovered that whenever $Z_{\text{D,white}}$ was in the range 1–2 m, the values of $Z_{\text{D,white}}(c + K_L)_{\text{phot}}$ tended to increase to 10–14, and consequently the few stations where $Z_{\text{D,white}} < 2$ m have been omitted. The reason for the discrepancy between theory and observations for small Secchi depths may be that one or more of the assumptions on which Eq. (21) is based becomes invalid. For instance, the assumption $L_{*\text{D}}(z) \approx L_*(z)$ made for Eq. (4) may be less good when Z_{D} is small. Figure 3 presents $(c + K_L)_{\text{phot}}$ as a function of $Z_{\text{D,white}}$ at the 32 stations where we have sufficient observations down to the Secchi depth, with the curve

$$(c + K_L)_{\text{phot}} = \frac{7.0}{Z_{\text{D,white}}} \tag{23}$$

added. The curve represents the mean value $(c + K_L)_{\text{phot}} Z_{\text{D,white}} = 7.0$, according to Table 3. It has been extended to values of $Z_{\text{D,white}} < 2$ m to illustrate that it will significantly underestimate $(c + K_L)_{\text{phot}}$ in this range. The symbol $R^2 = 0.87$ in Fig. 3 is the coefficient of determination. The general definition of this quantity for a data set (x, y) and a chosen trendline $f(x)$ is $R^2 = 1 - (\varepsilon^2/s_y^2)$, where ε is the root mean square of the residuals $y - f(x)$, and s_y is the standard deviation of y. It should be pointed out that while the quantity R^2 depends on the chosen trendline, the coefficient of correlation r is solely a function of the data set (x, y), since r is defined by $r = S_{x,y}/(s_x s_y)$, where $S_{x,y}$ is the covariance of x and y, and s_x is the standard deviation of x.

Another way to test the mean value ln(A) = 7.3 in Eq. (21) is to correlate $(c + K_L)_{\text{phot}}$ with $1/Z_{\text{D,white}}$. The best-fit line through the origin obtains the slope 7.5, and if $(c + K_L)_{\text{phot}}$ is estimated by $7.5/Z_{\text{D,white}}$, the rms of the error $[(c + K_L)_{\text{phot}} - 7.5/Z_{\text{D,white}}]$ becomes 0.23 m^{-1}. The mean value of $(c + K_L)_{\text{phot}}$ is 1.09 m^{-1} (Table 3), and the rms error relative to this value represents 21 %. It is interesting that if we estimate $(c + K_L)_{\text{phot}}$ by using Eq. (23), the rms error only changes to 0.24 m^{-1} or 22 %. The coefficient of determination in this case becomes $R^2 = 0.88$.

If the observer's eye is below the surface, $\bar{\rho}_{L,\text{air}} = 0$ and $W = 1$, and the value of ln(A) in Eq. (21) becomes 8.7. Tyler (1968) estimated the number 8.69 for this case, while Holmes (1970) found for sub-surface observations in turbid coastal waters that the average value of $Z_{\text{D,white}}(c + K_L)_{\text{phot}}$ was 9.4. Højerslev (1977) obtained the same value for the sub-surface case. Thus our theoretical estimate of ln(A) for the sub-surface case agrees with Tyler, but deviates 8 % from the estimates by Holmes and Højerslev. Højerslev (1977) found that for observations above the surface, the product $Z_{\text{D,white}}(c + K_L)_{\text{phot}}$ should be in the range 7.9–9.4. This is 8–29 % above our estimate in Table 3.

4.5 Effect of colour filters and the black disk

When the white Secchi disk is observed through the coloured glass filters, the optical coefficients and ln(A) change values, as shown by Table 3. The table demonstrates that in this case the observed mean values of $Z_{\text{D}}(c + K_L)_{\text{phot}}$ are more than 30 % smaller than the estimated mean values of ln(A).

The best-fit correlation lines $y = A + Bx$ and $y = B_0 x$ for the observations of $Z_{\text{D,blue}}$, $Z_{\text{D,green}}$ and $Z_{\text{D,red}}$ as functions of $Z_{\text{D,white}}$ have been determined, and the found constants A, B and B_0 as well as the mean values of the ratios $(y/x) = Z_{\text{D,filter}}/Z_{\text{D,white}}$ are presented in Table 4. We see that the colour filters reduce the Secchi depths to 50–70 % of the depths for the open eye. The result that $Z_{\text{D,green}}$ on average is reduced to almost 70 % of $Z_{\text{D,white}}$, although the wavelengths of peak photopic sensitivity for $Z_{\text{D,green}}$ and $Z_{\text{D,white}}$ are very close (Table 2), may be due to the half-peak bandwidth of the green filter, which is only half of that for the open eye.

Table 4 also shows the correlation lines $y = A + Bx$ with the constant term A. When the values of B_0, B and $(y/x)_{\text{mean}}$ are close to each other, it means that the observations lie close to a straight line through the origin.

Mikaelsen and Aas (1990) observed the Secchi depth in the Inner Oslofjord during 1986–1987. Based on their data from 11 stations the mean values of the ratio $Z_{\text{D,filter}}/Z_{\text{D,white}}$ become 0.61, 0.81 and 0.62 for the blue, green and red filter,

Table 4. Linear relationships of the forms $y = A + Bx$ and $y = B_0x$ obtained by correlation analysis of Z_D (white disk) observed by the open eye and with blue, green and red glass filters, and $Z_{D,black}$ (disk) and $Z_{B,black}$ (bowl) observed by the open eye. Mean values of y/x and y and their standard deviations are included. The size of the disk is 30 cm if not otherwise indicated. r is the correlation coefficient, ε is the root-mean-square error of the deviations (y–A–Bx), and ε_0 is the rms of (y–B_0x). N is the number of data pairs (y, x).

y [m]	x [m]	r	A [m]	B	B_0	$(y/x)_{mean\pm sd}$	$y_{mean\pm sd}$ [m]	ε [m]	ε_0 [m]	N
$Z_{D,blue}$	$Z_{D,white}$	0.89	0.2	0.49	0.52	0.53 ± 0.10	4.0 ± 1.6	0.7	0.7	25
$Z_{D,green}$	$Z_{D,white}$	0.96	−0.5	0.79	0.73	0.71 ± 0.09	5.5 ± 2.4	0.7	0.7	25
$Z_{D,red}$	$Z_{D,white}$	0.94	0.5	0.48	0.54	0.56 ± 0.08	4.2 ± 1.5	0.5	0.5	25
$Z_{B,black}$	$Z_{D,black}$	0.63	0.8	0.77	1.20	1.29 ± 0.44	2.2 ± 0.7	0.5	0.5	19
$Z_{B,black}$	$Z_{D,white}$	0.11	1.9	0.03	0.23	0.26 ± 0.11	2.2 ± 0.7	0.7	0.9	19
$Z_{D,black}$	$Z_{D,white}$	0.54	0.8	0.17	0.26	0.29 ± 0.10	2.2 ± 0.9	0.8	0.8	50
$Z_{D,white,10}$	$Z_{D,white,30}$	0.99	−0.4	0.85	0.81	0.80 ± 0.06	6.9 ± 2.8	0.5	0.5	21
$Z_{D,blue,10}$	$Z_{D,blue,30}$	0.98	−0.1	0.91	0.90	0.88 ± 0.08	3.2 ± 1.5	0.3	0.3	13
$Z_{D,green,10}$	$Z_{D,green,30}$	0.94	1.0	0.70	0.83	0.87 ± 0.12	5.3 ± 2.5	0.8	0.9	13
$Z_{D,red,10}$	$Z_{D,red,30}$	0.95	0.1	0.88	0.90	0.91 ± 0.10	3.9 ± 1.5	0.4	0.4	13
$Z_{D,all,10}$	$Z_{D,all,30}$	0.98	0.4	0.78	0.83	0.86 ± 0.10	5.1 ± 2.7	0.6	0.6	60
$Z_{D,white,shade}$	$Z_{D,white,sun}$	0.96	−0.2	0.99	0.97	0.97 ± 0.10	8.3 ± 3.3	0.9	0.9	34
$Z_{D,blue,shade}$	$Z_{D,blue,sun}$	0.91	0.5	0.74	0.83	0.87 ± 0.15	4.1 ± 1.8	0.7	0.8	29
$Z_{D,green,shade}$	$Z_{D,green,sun}$	0.94	0.1	0.90	0.91	0.91 ± 0.12	5.6 ± 2.6	0.9	0.9	29
$Z_{D,red,shade}$	$Z_{D,red,sun}$	0.85	0.4	0.82	0.89	0.91 ± 0.16	4.0 ± 1.4	0.7	0.8	29
$Z_{D,all,shade}$	$Z_{D,all,sun}$	0.95	−0.2	0.96	0.93	0.91 ± 0.14	5.6 ± 3.0	0.9	0.9	121
$Z_{D,white,10,tel}$	$Z_{D,white,10}$	0.96	−1.0	1.37	1.22	1.14 ± 0.20	7.2 ± 3.8	1.1	1.2	15
$Z_{D,blue,10,tel}$	$Z_{D,blue,10}$	0.93	−0.1	1.18	1.15	1.14 ± 0.18	3.3 ± 1.8	0.6	0.6	11
$Z_{D,green,10,tel}$	$Z_{D,green,10}$	0.96	−0.7	1.27	1.15	1.09 ± 0.15	5.2 ± 2.9	0.7	0.8	11
$Z_{D,red,10,tel}$	$Z_{D,red,10}$	0.92	0.1	1.14	1.15	1.16 ± 0.18	4.2 ± 1.8	0.7	0.7	11
$Z_{D,all,10,tel}$	$Z_{D,all,10}$	0.96	−0.5	1.28	1.19	1.14 ± 0.18	5.2 ± 3.1	0.9	0.9	48

respectively, which is 11–15 % greater than our results of 0.53, 0.73 and 0.54 in Table 4. Both the first and the latter set of values resemble Lisitzin's results from the Baltic Sea (1938) when $Z_{D,white} < 10$ m. In the clear and blue waters of the Florida Shelf where $Z_{D,white}$ was 21–26 m, Højerslev's colour filter observations (1985) yielded mean values of the ratios equal to 0.90, 0.91 and 0.29 for the blue, green and red filters. The difference from our results in greenish coastal waters is clearly a result of the difference in water colour.

Table 3 predicts that the average value of $Z_{D,black}(c + K_L)_{phot}$ should be $\ln(A) = 4.7$ for the 30 cm black disk, but the observed value is less than half of this: 1.9. This could be because an ordinary disk of black plastic was used in these observations, and not the bowl-shaped device. The surface of the plastic disk seemed to be entirely black on deck, but looked dark grey in the sea, and brighter than its background. In 1992 a series of measurements at 19 stations was taken with the black-painted bowl together with the black and white disks. The depth $Z_{B,black}$ of the black bowl was on average 20–30 % greater than the depth $Z_{D,black}$ of the black disk (Table 4). Thus the bowl produces a smaller reflection and a greater contrast than the disk. Since the estimated attenuation $(c + K_L)_{phot}$ is approximately the same for the black and white disks as shown by Table 3 (the minor difference being due to $Z_{D,black}$ being smaller than $Z_{D,white}$), the values of $\ln(A)$ in Table 3 imply that the ratio $Z_{B,black}/Z_{D,white}$ should be approximately $4.7/7.3 = 0.64$. However, the observed ratio in Table 4 is only 0.23–0.26. This could mean that our black bowl is not perfectly black, but it could also be that the use of colour filters and the black disk or bowl introduces effects that are not included in Eq. (21).

4.6 Effect of size

The observations with the 10 cm disks were made in 1992, when instruments for spectral recordings of c and K_L were not available. Consequently the two sides of Eq. (21) cannot be tested directly for the 10 cm disk, but other experiments have been made. The angle α of the total field of view across the 10 cm Secchi disk can be calculated from Eq. (22) with $D = 0.1$ m, $H = 3$ m and $n = 1.33$. Because the observed values of Z_D for this smaller disk lie in the interval from 0.5 to 12 m, the angle α across the Secchi disk becomes 0.5°–1.7°. The threshold contrast for the smaller disk becomes greater than for the 30 cm disk, while the value of W will be reduced according to Eq. (14), because D^2 is reduced more than Z_D^2. The combined effect is that the values of $\ln(A)$ in Table 3 for the 30 cm white and black disks will be reduced by 22 and 13 %, respectively. For the blue, green and red colour filters the decreased size produces similar reductions of 18, 21, and 17 %. This can be tested directly by comparing the values of Z_D for disk diameters of 10 and

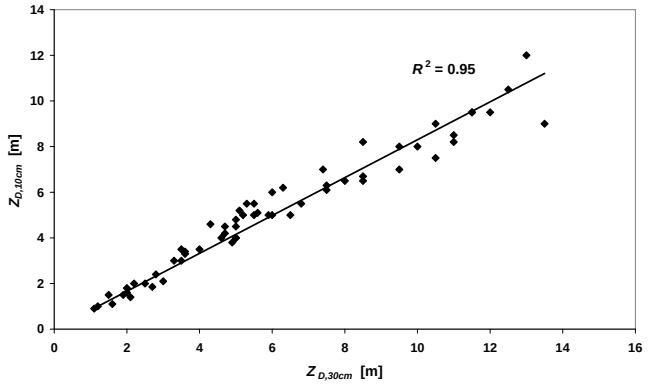

Fig. 4. All naked eye and colour filter observations of Z_D with a 10 cm disk as a function of the observations with a 30 cm disk. The best-fit line through the origin is the function $Z_{D,10\ cm} = 0.83\, Z_{D,30\ cm}$.

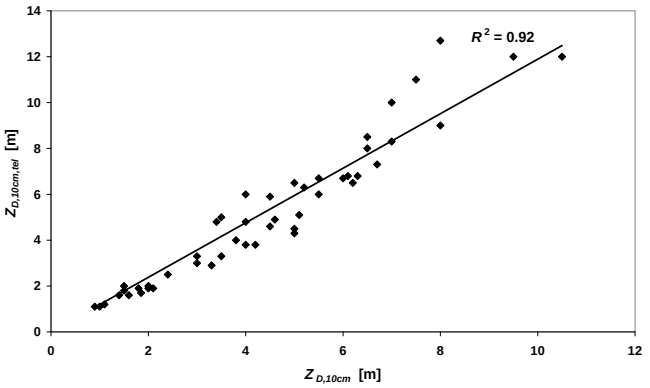

Fig. 5. All naked eye and colour filter observations of $Z_{D,10\ cm,tel}$ with a telescope as a function of $Z_{D,10\ cm}$ without a telescope. The best-fit line through the origin is the function $Z_{D,10\ cm,tel} = 1.19 Z_{D,10\ cm}$.

30 cm. The results in Table 4 show that the relative influence of size is greater for the open eye than for the colour filters, and that the decrease in diameter from 30 to 10 cm reduces the Secchi depth by an average of 10–20 %, in agreement with our estimates. Figure 4 presents all open-eye and colour filter observations for 10 and 30 cm disks put together, and the best fit line through the origin obtains a slope of 0.83, indicating an average Secchi depth reduction of 17 %.

4.7 Effects of sun glitter, water telescope and ship shadow

The effect of a water telescope is to eliminate sun glitter and skylight reflection at the surface, and to reduce the blurring effect of capillary waves. If we insert a surface reflectance $\bar{\rho}_{L,\mathrm{air}} = 0$ and a wave factor $W = 1$ into Eq. (21), we find that $\ln(A)$ should increase by 12 % for the 30 cm white disk, based on the estimated quantities in Table 3. For the colour filters and black disk the effect is in the range ± 6 %. Mikaelsen and Aas (1990) tested the effect at four stations in 1987 with a 30 cm disk. According to their observations $Z_{\mathrm{D,white}}$ increased by 11 % on average using the water telescope, and by including the observations with the colour filters the increase became 15 %. New experiments were done in 1992, and a 10 cm disk was used in order to see it properly within the field of view of the telescope. The results, listed in the last five rows of Table 4, show that the telescope increased $Z_{\mathrm{D,white,10}}$ by an average of 14 %, and the effect on $Z_{\mathrm{D,filter,10}}$ was of the same magnitude. If all open-eye and filter observations are put together (Table 4), we see that the average increase in the Secchi depth by using the telescope is the same, 14 %. The best-fit line through the origin obtains the slope 1.19 (Fig. 5), indicating an average increase of 19 %.

Holmes' use of a water telescope (1970) only increased the observed depth by 2–4 %, which is significantly less than our result. Højerslev (1986) found for Baltic waters that the ratio between the depth $Z_{\mathrm{D,tel}}$ observed with a water telescope and the ordinary Z_D could be approximated by a function of the wave height H in units of metres: $Z_{\mathrm{D,rel}}/Z_D = 1 + 0.4\, H$. This expression underestimates the effect at our 11 water telescope stations where H was < 0.1 m, but we have not tested it in more rough seas. Sandén and Håkansson (1996) investigated the effect of wind on Z_D, and it seems like the presence of wind tended to reduce the depth by ~ 10 %.

If we observe the Secchi disk on the sunlit side of the ship, sun glitter from the sea will reduce its threshold depth. On the shadow side there may be less glitter, but the ship shadow will also reduce the luminances from both the background and the disk, and this may require a greater contrast, and thus lead to a smaller depth. The balance between gains and losses related to the absence or presence of direct sunlight is demonstrated by Fig. 6, which presents the Secchi depths observed on both sides of the ship with the white disk. The best-fit line through the origin obtains the slope 0.97, which is close to 1. If we do the same experiment for all depths observed with colour filters and the open eye (Table 4), we see that the slope becomes 0.93, that is Z_D is now on average reduced by 7 % on the shadow side.

4.8 The monochromatic assumption

In Sect. 2 it was assumed as a first approximation that the beam attenuations of the upward luminances resembled the attenuations of the radiances at the wavelength of maximum spectral transmittance, and Sect. 4.1 described how the efficient attenuation coefficients $c_{\mathrm{phot,disk}}$ and c_{phot} of upward luminance from the disk and background could be estimated. In this section we will investigate the relationships between the photopic and monochromatic coefficients as well as the errors introduced by the monochromatic assumption.

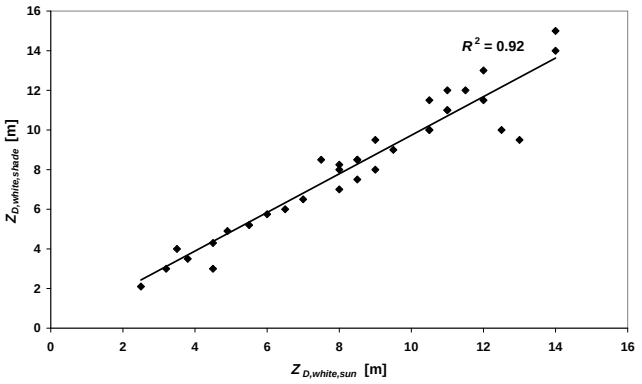

Fig. 6. All naked eye and colour filter observations of Z_D, on the shaded versus the sunlit side of the ship. The best-fit line through the origin is the function $Z_{D,shade} = 0.93 Z_{D,sun}$.

The coefficients $c_{phot,disk}$ and c_{phot} have been correlated with the monochromatic beam attenuation coefficient c_{555} at 555 nm, and the results are presented in Table 5. Similarly, the vertical attenuation coefficient $K_{L,phot}$ has been correlated with $K_{L,555}$. The correlations are described by best-fit lines on the forms $y = A + Bx$ and $y = B_0 x$. Table 5 also displays values of $(y/x)_{mean}$ and y_{mean}. We see that the values of B, B_0 and $(y/x)_{mean}$ are close to each other, indicating that the points (x, y) lie close to the lines. This is confirmed by the very small errors ε and ε_0 introduced by using the correlation lines ($\approx 0.01\,m^{-1}$). ε and ε_0 are defined as the root mean squares of the deviations $(y–A–Bx)$ and $(y–B_0x)$, respectively. The coefficient c_{phot}, for instance, is almost identical to c_{555}, with an average ratio of 1.02. However, Table 5 also demonstrates that the deviations between the photic and monochromatic coefficients are greatest for $K_{L,phot}$ versus $K_{L,555}$, which displays a slope of 1.12. The sum $(c+K_L)_{phot}$ versus $(c + K_L)_{555}$ obtains the slope 1.03.

It follows from the descriptions of c_{phot} and $K_{L,phot}$ that these coefficients are apparent optical properties, depending on the ambient light field. It could not be stated a priori that they would be so strongly correlated with the monochromatic coefficients at 555 nm, with a coefficient of correlation equal to 1.00. We have not investigated how the found relationships will work in more clear and bluish sea waters, but we assume that the correlations may be weaker there. Holmes (1970) equipped his irradiance and beam attenuation meters with filters where the spectral shape of the transmittance resembled the spectral sensitivity of the eye, but the attenuation meter then recorded a lamp spectrum that probably was different from the natural spectrum within the sea.

The correlation results for attenuation coefficients derived from luminances observed through the colour filters (Table 5) versus monochromatic coefficients show that the correlation coefficients are all very close to 1.0. The slope B_0 for the blue and green filters obtains values between 0.95 and 1.01, while the red filter deviates more from 1.0 with the slopes 1.06 and 1.21. The slopes B_0 for the sum $(c + K_L)$ are in the range 0.97–1.10. None of these deviations from the slope 1.0 explain the discrepancies between theory and observations displayed by Table 3 for the colour filters. Our overall conclusion becomes that the monochromatic assumption works satisfactorily, and that the mentioned discrepancies must have other causes. In Blackwell's experiments (1946) the targets were projections of "white" light from electrical lamps onto a white screen. The different parts of the visible spectrum were not investigated separately, and it could perhaps be that C_t also has a spectral dependence.

It remains to test the ability of Eq. (21) to describe the relationships between Z_D and monochromatic values of c, K_L and $(c + K_L)$. This will be done in the next section.

5 Relationships between the Secchi depth and other quantities

5.1 Estimates of monochromatic coefficients

In Sect. 2 we assumed that the Secchi depth observed with the open eye might be determined by the attenuation coefficients at the wavelength of maximum water transmittance, that is around 555 nm. Section 4.4 demonstrated that the numerical values of the constants in the relationships between Z_D and $(c + K_L)$ would depend on the chosen method. If our intention is to estimate $(c + K_L)_{555}$ from observed $Z_{D,white}$, the obvious choice, based on the form of Eq. (21), is to perform a linear correlation analysis between $(c + K_L)_{555}$ and $1/Z_{D,white}$. The slope of the line through the origin obtains the value 7.4, which is practically the same as the slope 7.5 found in Sect. 4.4 for $(c + K_L)_{phot}$. However, usually in marine-optical research the singular values of c and K_L are more interesting than their sum $(c + K_L)$, and therefore c_{555} and $K_{L,555}$ have been separately correlated with $1/Z_{D,white}$, as shown by Table 6. While the correlation coefficient is 0.95 for c_{555}, which is almost as perfect as it can be expected to be, it is reduced to 0.72 for $K_{L,555}$. Similar results have been obtained for the channels at 412, 443, 490, 510, 620 and 665 nm (Table 6). The root-mean-square errors of K_L and c, estimated from the correlation lines, are in the range $0.1–0.6\,m^{-1}$, but because K_L is smaller than c the relative errors become greater for K_L than for c. The result that the correlation coefficients are greater for c than for K_L is as expected since c contributes more than K_L to the sum $(c + K_L)$ which determines $Z_{D,white}$.

Often the vertical attenuation coefficient of downward irradiance, K_d, will be a more useful quantity than K_L. The correlation results for K_d at the MERIS channels as a function of $1/Z_{D,white}$ are presented in Table 6. Some of the values are remarkably similar to those obtained for K_L, and the reason for this is that the mean value of the ratio K_d/K_L usually is close to 1. In order to complete the investigation, the coefficient K_u of upward irradiance has been included in

Table 5. Linear relationships of the forms $y = A + Bx$ and $y = B_0x$ obtained by correlation analysis of attenuation coefficients of spectrally integrated luminance for the open eye and with blue, green and red glass filters and coefficients of monochromatic radiance at 470, 540, 555 and 620 nm, and mean values of y/x and y. The attenuation coefficients are averages over the depth range $0–Z_{D,white}$. r is the correlation coefficient. The error ε is the root mean square of the deviations ($y–A–Bx$), and ε_0 is the rms of ($y - B_0x$). The analysis is based on 32 stations.

y [m^{-1}]	x [m^{-1}]	r	A [m^{-1}]	B	B_0	$(y/x)_{mean\pm sd}$	$y_{mean\pm sd}$ [m^{-1}]	ε [m^{-1}]	ε_0 [m^{-1}]
$c_{phot,disk}$	c_{555}	1.00	0.02	0.99	1.01	1.02 ± 0.01	0.83 ± 0.50	0.01	0.02
c_{phot}	c_{555}	1.00	0.01	1.00	1.01	1.02 ± 0.01	0.83 ± 0.51	0.01	0.01
$K_{L,phot}$	$K_{L,555}$	1.00	0.00	1.12	1.12	1.11 ± 0.05	0.26 ± 0.19	0.01	0.01
$(c + K_L)_{phot}$	$(c + K_L)_{555}$	1.00	0.00	1.03	1.03	1.03 ± 0.01	1.09 ± 0.67	0.01	0.01
$c_{phot,blue}$	c_{470}	1.00	0.06	0.90	0.95	0.98 ± 0.04	0.97 ± 0.65	0.04	0.05
$c_{phot,green}$	c_{540}	1.00	0.02	0.97	0.98	1.00 ± 0.01	0.83 ± 0.52	0.01	0.02
$c_{phot,red}$	c_{620}	1.00	0.18	0.91	1.06	1.12 ± 0.07	1.03 ± 0.41	0.03	0.08
$K_{L,phot,blue}$	$K_{L,470}$	0.99	0.05	0.95	1.01	1.10 ± 0.05	0.44 ± 0.36	0.04	0.05
$K_{L,phot,green}$	$K_{L,540}$	1.00	0.01	0.96	0.98	1.00 ± 0.01	0.25 ± 0.18	0.00	0.01
$K_{L,phot,red}$	$K_{L,620}$	0.99	0.09	1.05	1.21	1.27 ± 0.08	0.45 ± 0.18	0.02	0.04
$(c + K_L)_{phot,blue}$	$(c + K_L)_{470}$	1.00	0.11	0.92	0.97	1.02 ± 0.04	1.41 ± 0.99	0.07	0.09
$(c + K_L)_{phot,green}$	$(c + K_L)_{540}$	1.00	0.03	0.96	0.98	1.00 ± 0.01	1.08 ± 0.67	0.01	0.02
$(c + K_L)_{phot,red}$	$(c + K_L)_{620}$	1.00	0.25	0.94	1.10	1.16 ± 0.07	1.48 ± 0.56	0.04	0.11

Table 6. Relationships of the forms $y = A + Bx$ and $y = B_0x$, where A, B and B_0 are coefficients from the correlation analysis between y and $x = 1/Z_{D,white}$. The error ε is the root mean square of the deviations ($y–A–Bx$), and ε_0 is the rms of ($y–B_0x$). r is the correlation coefficient and N is the number of stations.

y [m^{-1}]	r	A [m^{-1}]	B	B_0	$(y/x)_{mean\pm sd}$	$y_{mean\pm sd}$ [m^{-1}]	ε [m^{-1}]	ε_0 [m^{-1}]	N
c_{412}	0.86	−0.24	10.6	9.6	8.8 ± 2.3	1.67 ± 1.20	0.58	0.60	79
c_{443}	0.91	−0.23	9.0	8.0	7.2 ± 1.7	1.38 ± 0.97	0.37	0.39	79
c_{490}	0.94	−0.22	7.6	6.6	6.0 ± 1.2	1.14 ± 0.79	0.22	0.28	79
c_{510}	0.95	−0.21	7.2	6.4	5.7 ± 1.1	1.10 ± 0.75	0.20	0.26	79
c_{555}	0.95	−0.17	6.6	5.9	5.4 ± 1.0	1.02 ± 0.68	0.18	0.20	79
c_{620}	0.95	0.03	6.1	6.3	6.3 ± 0.9	1.14 ± 0.63	0.18	0.18	79
c_{665}	0.93	0.18	5.8	6.5	6.9 ± 1.1	1.21 ± 0.60	0.19	0.21	79
$K_{L,412}$	0.66	0.01	4.6	4.6	4.5 ± 1.8	0.91 ± 0.77	0.57	0.57	53
$K_{L,443}$	0.64	−0.05	4.2	4.0	3.7 ± 2.0	0.78 ± 0.72	0.55	0.55	53
$K_{L,490}$	0.72	−0.02	2.4	2.3	2.2 ± 0.9	0.45 ± 0.36	0.25	0.25	53
$K_{L,510}$	0.72	0.00	2.0	2.0	1.9 ± 0.7	0.39 ± 0.30	0.21	0.21	53
$K_{L,555}$	0.72	0.05	1.3	1.5	1.6 ± 0.5	0.31 ± 0.20	0.14	0.14	53
$K_{L,620}$	0.77	0.15	1.5	2.1	2.4 ± 0.7	0.45 ± 0.22	0.14	0.15	53
$K_{L,665}$	0.78	0.22	1.7	2.5	3.0 ± 0.8	0.55 ± 0.24	0.15	0.18	53
$K_{d,412}$	0.59	−0.02	5.9	5.8	5.4 ± 3.3	1.14 ± 1.11	0.89	0.89	53
$K_{d,443}$	0.64	−0.05	4.2	4.0	3.7 ± 2.0	0.78 ± 0.72	0.55	0.55	53
$K_{d,490}$	0.70	−0.03	2.5	2.4	2.2 ± 1.0	0.46 ± 0.39	0.28	0.28	53
$K_{d,510}$	0.71	−0.02	2.1	2.0	1.9 ± 0.8	0.40 ± 0.32	0.22	0.22	53
$K_{d,555}$	0.74	0.02	1.4	1.5	1.5 ± 0.5	0.30 ± 0.21	0.14	0.14	53
$K_{d,620}$	0.82	0.25	1.2	2.2	2.8 ± 0.8	0.49 ± 0.16	0.09	0.15	53
$K_{d,665}$	0.86	0.41	1.1	2.7	3.7 ± 1.2	0.62 ± 0.13	0.07	0.21	53
$K_{u,412}$	0.43	0.18	6.5	7.2	7.0 ± 6.5	1.42 ± 1.61	1.43	1.43	51
$K_{u,443}$	0.52	0.05	5.2	5.4	5.1 ± 3.5	1.05 ± 1.08	0.92	0.92	51
$K_{u,490}$	0.67	−0.03	3.1	3.0	2.8 ± 1.4	0.58 ± 0.51	0.38	0.38	53
$K_{u,510}$	0.68	0.00	2.5	2.5	2.4 ± 1.1	0.50 ± 0.41	0.30	0.30	53
$K_{u,555}$	0.64	0.06	1.6	1.9	2.0 ± 0.8	0.38 ± 0.28	0.21	0.22	53
$K_{u,620}$	0.71	0.20	1.9	2.7	3.1 ± 1.1	0.58 ± 0.29	0.21	0.23	53
$K_{u,665}$	0.72	0.30	2.1	3.3	3.9 ± 1.3	0.71 ± 0.32	0.22	0.26	53

Table 7. Relationships of the forms $y = A + Bx$ and $y = B_0x$ obtained by correlation analysis of attenuation coefficients of monochromatic radiance and irradiance and Secchi depths observed with the open eye and with blue, green and red glass filters. The attenuation coefficients are averages over the depth range $0–Z_{D,white}$, and r is the correlation coefficient. The error ε is the root mean square of the deviations ($y–A–Bx$), and ε_0 is the rms of ($y–B_0x$). The analysis is based on 25 stations.

y [m^{-1}]	x [m^{-1}]	r	A [m^{-1}]	B	B_0	$(y/x)_{mean\pm sd}$	$y_{mean\pm sd}$ [m^{-1}]	ε [m^{-1}]	ε_0 [m^{-1}]
c_{470}	$1/Z_{D,blue}$	0.84	−0.23	4.3	3.7	3.4 ± 1.1	1.09 ± 0.79	0.42	0.43
c_{470}	$1/Z_{D,white}$	0.94	−0.34	9.0	7.3	6.4 ± 1.6	1.09 ± 0.79	0.26	0.30
c_{540}	$1/Z_{D,green}$	0.94	−0.12	4.5	4.1	3.9 ± 0.9	0.91 ± 0.59	0.19	0.20
c_{540}	$1/Z_{D,white}$	0.96	−0.18	6.9	5.9	5.5 ± 1.1	0.91 ± 0.59	0.15	0.17
c_{620}	$1/Z_{D,red}$	0.89	0.24	2.6	3.3	3.6 ± 0.7	1.00 ± 0.49	0.22	0.25
c_{620}	$1/Z_{D,white}$	0.97	0.09	5.7	6.2	6.4 ± 0.9	1.00 ± 0.49	0.12	0.13
$K_{L,470}$	$1/Z_{D,blue}$	0.74	−0.17	2.0	1.6	1.4 ± 0.7	0.45 ± 0.42	0.28	0.29
$K_{L,470}$	$1/Z_{D,white}$	0.80	−0.20	4.1	3.1	2.6 ± 1.2	0.45 ± 0.42	0.25	0.26
$K_{L,540}$	$1/Z_{D,green}$	0.79	−0.04	1.3	1.2	1.2 ± 0.4	0.27 ± 0.21	0.13	0.13
$K_{L,540}$	$1/Z_{D,white}$	0.80	−0.06	2.0	1.7	1.6 ± 0.6	0.27 ± 0.21	0.12	0.13
$K_{L,620}$	$1/Z_{D,red}$	0.80	0.11	0.9	1.2	1.4 ± 0.4	0.38 ± 0.19	0.11	0.13
$K_{L,620}$	$1/Z_{D,white}$	0.83	0.07	1.9	2.3	2.5 ± 0.6	0.38 ± 0.19	0.10	0.11
$K_{d,470}$	$1/Z_{D,blue}$	0.73	−0.17	2.0	1.6	1.4 ± 0.7	0.44 ± 0.42	0.29	0.29
$K_{d,470}$	$1/Z_{D,white}$	0.82	−0.21	4.1	3.0	2.6 ± 1.2	0.44 ± 0.42	0.24	0.26
$K_{d,540}$	$1/Z_{D,green}$	0.80	−0.05	1.3	1.2	1.1 ± 0.4	0.26 ± 0.20	0.12	0.12
$K_{d,540}$	$1/Z_{D,white}$	0.81	−0.06	2.0	1.7	1.6 ± 0.5	0.26 ± 0.20	0.12	0.12
$K_{d,620}$	$1/Z_{D,red}$	0.80	0.26	0.62	1.3	1.7 ± 0.4	0.44 ± 0.13	0.07	0.15
$K_{d,620}$	$1/Z_{D,white}$	0.83	0.23	1.3	2.4	3.1 ± 0.8	0.44 ± 0.13	0.07	0.13
$K_{u,470}$	$1/Z_{D,blue}$	0.72	−0.34	3.1	2.2	1.8 ± 1.0	0.60 ± 0.65	0.44	0.47
$K_{u,470}$	$1/Z_{D,white}$	0.78	−0.38	6.2	4.3	3.4 ± 2.0	0.60 ± 0.65	0.39	0.43
$K_{u,540}$	$1/Z_{D,green}$	0.80	−0.06	1.6	1.4	1.4 ± 0.5	0.31 ± 0.25	0.15	0.15
$K_{u,540}$	$1/Z_{D,white}$	0.80	−0.07	2.4	2.0	1.9 ± 0.7	0.31 ± 0.25	0.15	0.15
$K_{u,620}$	$1/Z_{D,red}$	0.77	0.17	1.0	1.5	1.7 ± 0.5	0.47 ± 0.22	0.14	0.16
$K_{u,620}$	$1/Z_{D,white}$	0.82	0.12	2.2	2.8	3.1 ± 1.0	0.47 ± 0.22	0.13	0.14

Table 6. The results indicate that the errors of the estimated vertical coefficients are greatest for K_u and smallest for K_L, and less in the green and red part of the spectrum than in the blue part. We suspect that the rms errors at 412 and 443 nm of 90–100 % are due to varying amounts of yellow substance which will influence the coefficients more than the Secchi depth. In addition weak signals compared to noise and detection level at these wavelengths create errors.

Gordon and Wouters (1978) found in their model study that in relatively turbid water, defined by the authors as water where the backscattering probability is constant, the product $cZ_{D,white}$ would be approximately constant, while $(c + K_d)Z_{D,white}$ would vary more. This result is in agreement with the results in Table 6.

In Table 6 the errors of the estimates produced by the best-fit lines $y = A + Bx$ and $y = B_0x$, where y is an attenuation coefficient and $x = 1/Z_{D,white}$, are shown. Usually the line $y = B_0x$ through the origin works satisfactorily, but at some wavelengths the addition of a constant term A reduces the error of the estimates significantly. Figure 7 shows observations of K_d at 555 and 665 nm versus $x = 1/Z_{D,white}$, together with the best-fit lines $y = A + Bx$. The value of A is 0.02 m^{-1} at 555 nm, and 0.41 m^{-1} at 665 nm (Table 6). It is interesting that Jerlov's K_d values for the clearest ocean water type I are of the same order of magnitude: 0.07 m^{-1} at 555 nm and 0.40 m^{-1} at 665 nm (e.g. Jerlov, 1976). Figure 7 indicates that in the green part of the spectrum the constant term can be omitted without any practical consequences, while in the red part a better fit is obtained if A is included. The inclusion of the constant term A reduces the error at 665 nm from 0.21 m^{-1} to 0.07 m^{-1} according to Table 6. For the vertical attenuation coefficients K_L and K_u of upward directed light the improvements by adding a constant term A to the correlation lines are less.

Mikaelsen and Aas (1990) analysed five stations in the Oslofjord with recordings of c, and 11 stations with K_d. Z_D was observed by the naked eye and with colour filters. Most of their results overlap with the present findings. Sørensen et al. (1993) obtained from 189 stations in the Oslofjord–Skagerrak area the mean value and standard deviation $c_{green}Z_{D,white} = 6.2 \pm 1.3$, which fall within the corresponding range of Table 6.

The relationships between the Secchi depths observed through the glass filters and the coefficients c, K_L, K_d and K_u at 470, 540 and 620 nm are presented in Table 7. The results, based on 25 stations, show that the errors of the estimated

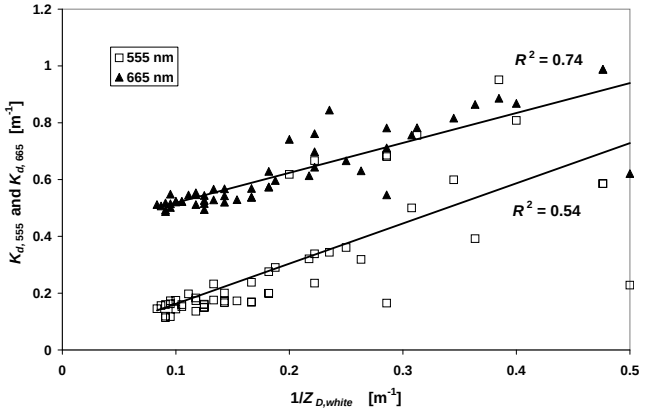

Fig. 7. K_d at 555 nm and 665 nm as a function of $1/Z_{D,white}$. The upper best-fit line is the function $K_{d,665} = [0.41\,m^{-1}] + 1.1/Z_{D,white}$ and the lower line is $K_{d,555} = [0.02\,m^{-1}] + 1.4/Z_{D,white}$.

coefficients are in the range 0.07–0.47 m^{-1}, or 10–80 % of the corresponding mean values. It is noteworthy that compared to the observations with the open eye, the colour filter observations represent no improvement in the accuracy of the estimated vertical attenuation coefficients. Especially for the coefficients of beam attenuation it is clear that $Z_{D,white}$ produces better estimates than $Z_{D,filter}$. We think this result is valid within our area of investigation, but not necessarily in other sea regions.

It may be noted that Table 7 contains analyses of attenuation coefficients at 620 nm that are parallel to those in Table 6, and that the results are different. The reason for this may be that Table 7 is based on stations with colour filter observations, and accordingly the number of applicable stations will be reduced to less than half of those in Table 6. Evidently the number of stations influences the statistical results.

Højerslev (1977) suggested the approximate mean values 3, 6 and 9 for the products $K_d Z_D$, cZ_D and $(c + K_d)Z_D$, respectively, where K_d, c and Z_D are observed through colour filters, but these findings are not confirmed by Table 7.

Because remote sensing of ocean colour is used to estimate coefficients like K_d, the technique can also be used to estimate the Secchi depth. Within our area of investigation the relationship between $1/Z_{D,white}$ and the water-leaving radiance L_w recorded in the red part of the spectrum (630–690 nm) by the TM3 sensor at the Landsat satellite was found to be $1/Z_{D,white} = [0.203\,m^{-1}] + [0.072\,W^{-1}\,m\,sr\,\mu m]L_w$, while the coefficient of correlation was 0.92 (Sørensen and Aas, 1994). For the TM1, TM2 and TM4 sensors in the blue-green (450–520 nm), green (520–600 nm) and near-infrared (760–900 nm) parts of the spectrum the coefficients of correlation became 0.69, 0.87 and 0.65, respectively. Kratzer et al. (2003) and Zhang et al. (2003) have discussed estimates of $1/Z_{D,white}$ based on satellite observation of the Baltic Sea, and Morel et al. (2007) have examined the Secchi depth estimates from various ocean colour sensors for the open ocean case. References to numerous investigations in lake waters can be found on the internet.

5.2 Quanta irradiance – PAR

The spectrally integrated quanta irradiance (400–750 nm), also termed PAR (photosynthetically available radiation), is one of several factors determining the primary production in the sea. If the transmittance of this irradiance between the surface and the Secchi depth is denoted T_D, then the average vertical attenuation coefficient K_q of the irradiance over the depth range $0 - Z_{D,white}$ is related to $Z_{D,white}$ by

$$T_D = e^{-K_q Z_{D,white}}. \quad (24)$$

The observed mean value ± the standard deviation of T_D, obtained from our third data set of 143 stations from the Oslofjord inside the Færder Light House at the Skagerrak border, is (9 ± 4) %. Based on the total data set of 205 stations, including stations from the nearby Skagerrak and Kattegat, the range becomes slightly greater: (9 ± 6) %.

Equation (24) can also be written as

$$K_q Z_{D,white} = -\ln(T_D), \quad (25)$$

and by using $T_D \approx 0.09 \pm 0.06$, the range of the product $K_q Z_{D,white}$ becomes 1.9–3.5. This is consistent with the mean value and standard deviation of the product obtained from observed pairs of K_q and $Z_{D,white}$: 2.5 ± 0.5 (Table 8). By linear correlation K_q may be estimated from $1/Z_{D,white}$ with an rms error that is less than 20 % of the mean value of K_q.

The depth of the euphotic zone, defined as the surface layer where there is a net positive production from photosynthesis, is often estimated as the depth $Z_q(1\,\%)$ where the quanta irradiance is reduced to 1 % of its surface value. If K_q is approximately constant with depth, $Z_q(1\,\%)$ can be determined from the equation

$$0.01 = e^{-K_q Z_q(1\,\%)} \quad (26)$$

which can be transformed to

$$Z_q(1\,\%) = \frac{4.61}{K_q}. \quad (27)$$

By inserting for K_q from Eq. (25), this expression becomes

$$Z_q(1\,\%) = \frac{4.61}{-\ln(T_D)}\, Z_{D,white}, \quad (28)$$

indicating a linear proportionality between $Z_q(1\,\%)$ and $Z_{D,white}$, provided $\ln(T_D)$ is approximately constant. Similar expressions can be deduced for $Z_q(3\,\%)$, $Z_q(10\,\%)$ and $Z_q(30\,\%)$.The correlation results for $Z_q(p\,\%)$ as a function of $Z_{D,white}$ are presented in Table 8, together with other related statistics.

Table 8. Linear relationships of the forms $y = A + Bx$ and $y = B_0 x$, obtained by correlation analysis of the vertical attenuation coefficient K_q of downward quanta irradiance, the depths $Z_q(p\,\%)$ where the quanta irradiance is reduced to p percent of the surface value, and the Secchi disk depth $Z_{D,white}$. The error ε is the root mean square of the deviations (y–A–Bx), ε_0 is the rms of (y–B_0x), and r is the correlation coefficient. The analysis is based on 205 stations.

y [m^{-1}]	x [m^{-1}]	r	A [m^{-1}]	B	B_0	$(y/x)_{mean\pm sd}$	$y_{mean\pm sd}$ [m^{-1}]	ε [m^{-1}]	ε_0 [m^{-1}]
K_q	$1/Z_{D,white}$	0.82	0.18	1.6	2.2	2.6 ± 0.7	0.52 ± 0.20	0.11	0.14
y [m]	x [m]	r	A [m]	B	B_0	$(y/x)_{mean\pm sd}$	$y_{mean\pm sd}$ [m]	ε [m]	ε_0 [m]
$Z_q(30\,\%)$	$Z_{D,white}$	0.72	1.0	0.22	0.36	0.44 ± 0.16	2.3 ± 0.8	0.6	0.7
$Z_q(10\,\%)$	$Z_{D,white}$	0.78	2.1	0.47	0.77	0.92 ± 0.30	4.9 ± 1.6	1.0	1.4
$Z_q(3\,\%)$	$Z_{D,white}$	0.79	3.5	0.79	1.3	1.5 ± 0.5	8.1 ± 2.7	1.7	2.2
$Z_q(1\,\%)$	$Z_{D,white}$	0.74	5.0	1.1	1.8	2.2 ± 0.7	11.5 ± 4.1	2.8	3.5
$Z_q(30\,\%)$	$Z_q(1\,\%)$	0.80	0.4	0.16	0.20	0.20 ± 0.04	2.3 ± 0.8	0.5	0.5
$Z_q(10\,\%)$	$Z_q(1\,\%)$	0.91	0.7	0.36	0.41	0.43 ± 0.06	4.9 ± 1.6	0.7	0.7
$Z_q(3\,\%)$	$Z_q(1\,\%)$	0.97	0.6	0.65	0.69	0.70 ± 0.05	8.1 ± 2.7	0.6	0.6

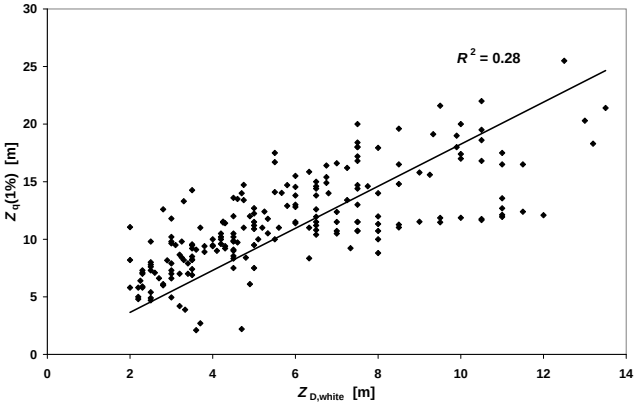

Fig. 8. The depth of the euphotic zone, estimated by the 1 % level $Z_q(1\,\%)$ of the surface quanta irradiance, as a function of the Secchi depth $Z_{D,white}$. The best-fit line through the origin is $Z_q(1\,\%) = 1.8\,Z_{D,white}$.

An old rule of thumb for the Oslofjord says that $Z_q(10\,\%)$ corresponds roughly to $Z_{D,white}$ (also suggested by Paulson and Simpson, 1977), and $Z_q(1\,\%)$ to twice this depth. We have already found that the average percentage of the quanta irradiance at $Z_{D,white}$ was 9 %, and when we calculate the average ratios $Z_q(10\,\%)/Z_{D,white}$ and $Z_q(1\,\%)/Z_{D,white}$, they become 0.9 and 2.2, respectively (Table 8). Figure 8 illustrates the significant scattering of points around the correlation line through the origin for $Z_q(1\,\%)$ as a function of $Z_{D,white}$. If we apply the relationship $y = A + Bx$ instead of the line through the origin, a slightly better fit is obtained, and the rms error for the estimates of $Z_q(1\,\%)$ as a function of $Z_{D,white}$ is reduced from 3.1 to 2.7 m (Table 8). Compared to the mean value 11.5 m of $Z_q(1\,\%)$, these numbers represent relative errors of 27 and 23 %, respectively.

Table 8 shows that estimates of Z_q from observed $Z_{D,white}$ are likely to have relative mean errors in the range 20–30 %. This is because $Z_{D,white}$ is primarily a function of $c + K_L$ (Eq. 20), while Z_q is a function of K_q only (Eq. 27). The vertical attenuation coefficients K_L and K_q are mainly functions of the absorption coefficient a, while the beam attenuation coefficient c consists of $a + b$, where b is the scattering coefficient. Thus Z_q is less influenced by particle scattering than Z_D, a property which reduces the correlation between the two quantities. It is our experience that an increased particle content in the sea may have a strong reducing effect on Z_D, while the influence on Z_q is much smaller. Still, the relationships in Table 8 will provide very useful checks of our irradiance measurements.

Not surprisingly the inter-correlations between $Z_q(1\,\%)$, $Z_q(3\,\%)$, $Z_q(10\,\%)$ and $Z_q(30\,\%)$ are stronger than between Z_q and $Z_{D,white}$ (Fig. 9). The statistical relationships are shown in Table 8.

Mikaelsen and Aas (1990) found $K_q Z_{D,white} = 2.7 \pm 0.6$, $Z_q(10\,\%) = 0.66\,Z_{D,white}$ and $Z_q(1\,\%) = 1.7\,Z_{D,white}$, while Sørensen et al. (1993) obtained $K_q Z_{D,white} = 2.3 \pm 0.4$. All of these results are close to the values in Table 8. Kratzer et al. (2003) found for Baltic waters that $K_q \approx 1.7/Z_{D,white}$, implying that for the same K_q the Secchi depth $Z_{D,white}$ tends to be greater in the Oslofjord than in the Baltic.

5.3 Chlorophyll *a* and total suspended material

The chlorophyll content is perhaps the most used concept when the amount of algae in the sea shall be described. Unfortunately the concentration of chlorophyll *a* (Chl) is not an optical property, although it influences the absorption and scattering coefficients of sea water. As a result our estimates obtained by correlation analysis of Chl as a function of $1/Z_D$, based on 41 stations north of 57.0° N, have average errors of

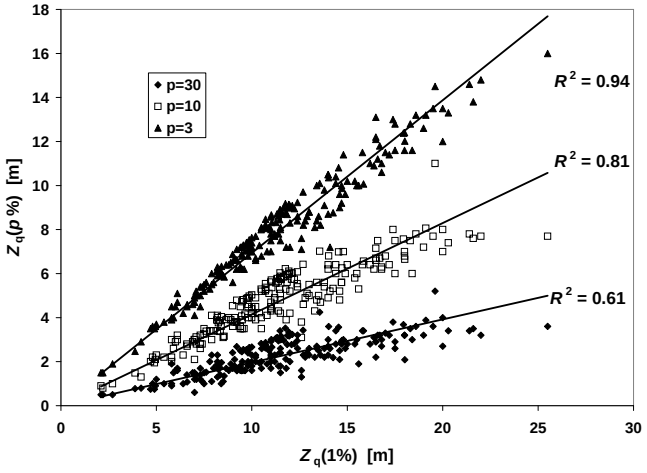

Fig. 9. The depth of the p % levels $Z_q(p\,\%)$ of the surface quanta irradiance, as a function of $Z_q(1\,\%)$ for p equal to 3, 10 and 30. The best-fit lines through the origin are $Z_q(3\,\%) = 0.69 Z_q(1\,\%)$, $Z_q(10\,\%) = 0.41 Z_q(1\,\%)$, and $Z_q(30\,\%) = 0.20 Z_q(1\,\%)$.

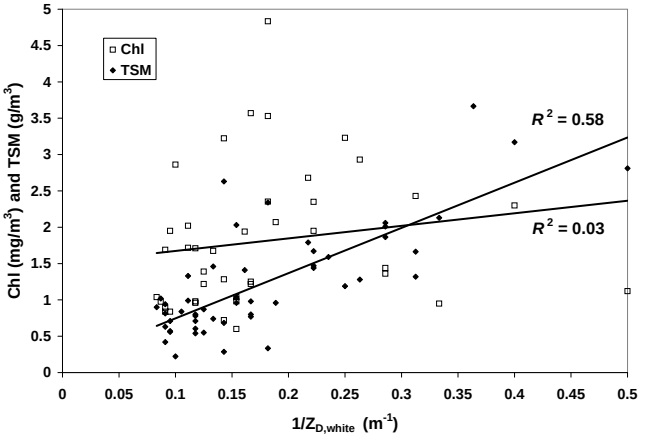

Fig. 10. Content of Chl and TSM versus $1/Z_{\mathrm{D,white}}$ at stations north of 57° N. The best-fit lines are $\mathrm{Chl} = [1.50\,\mathrm{mg\,m^{-3}}] + [1.73\,\mathrm{mg\,m^{-2}}]/Z_{\mathrm{D,white}}$ and $\mathrm{TSM} = [0.12\,\mathrm{g\,m^{-3}}] + [6.22\,\mathrm{g\,m^{-2}}]/Z_{\mathrm{D,white}}$.

50–90 % relative to the mean value of chlorophyll content (Table 9, Fig. 10). The estimates of total suspended material TSM (51 stations) for the same area have average errors of 40–70 % (Table 9, Fig. 10). Still, such relationships provide useful checks because they quantify the order of magnitude of the concentrations, within the area of investigation. Better correlations may sometimes be found for smaller regions. In general the relationships discussed in Sect. 5 are likely to show regional variations.

In the earlier investigation by Sørensen et al. (1993) the products $Z_{\mathrm{D,white}}$Chl (249 stations) and $Z_{\mathrm{D,white}}$ TSM (275 stations) obtained the mean values and standard deviations $(19 \pm 16)\,\mathrm{mg\,m^{-2}}$ and $(7.8 \pm 3.8)\,\mathrm{g\,m^{-2}}$, respectively, in agreement with the corresponding ranges of Table 9. An estimate of the product $Z_{\mathrm{D,white}}$Chl in the Baltic Sea, based on observations by Fleming-Lehtinen and Laamanen (2012), is $\sim 25\,\mathrm{mg\,m^{-2}}$.

The turbidity Turb, expressed in nephelometric formazine units (NFU), has not been included in the present study, because the accuracy of the corresponding turbidity data was not satisfactory. However, in the mentioned investigation by Sørensen et al. (1993) the mean value and standard deviation of the product $Z_{\mathrm{D,white}}$ Turb (308 stations) was $(3.5 \pm 1.4)\,\mathrm{m\,NFU^{-1}}$.

6 Summary and conclusions

We have analysed the Secchi depth Z_{D} and its relationship to other properties of the sea water in the Oslofjord–Skagerrak area. White and black disks of different sizes have been applied, and the Secchi depth has been observed with the naked eye, through colour filters and with a water telescope. A few stations where $Z_{\mathrm{D,white}}$ was less than 2 m or the Q factor was outside the range $\pi - 2\pi$ have been omitted. The upward luminance will typically have its spectral maximum in the green part of the spectrum, close to 555 nm.

An extended version of Tyler's equation for Z_{D}, as expressed by Eq. (21), has been tested. The right-hand side of the equation, $\ln(A)$, is a function of the reflectance $\bar{\rho}_{L,\mathrm{air}}$ at the air–sea interface, the reflectances $R_L(0)$ and $R_L(Z_{\mathrm{D}})$ of the sea water just below the surface and at the Secchi depth, the reflectance ρ_{DL} of the disk, the contrast threshold C_{t} of the human eye, the contrast transmittance W through the surface and the factor $\mathfrak{R}$. With the estimated mean values for these quantities (Table 3), $\ln(A)$ obtains the mean value $\pm$ the standard deviation 7.3 ± 0.9 for the 30 cm white disk observed with the naked eye. The left-hand side of the equation is the product of the observed Secchi depth $Z_{\mathrm{D,white}}$ and the attenuation coefficients $(c + K_L)_{\mathrm{phot}}$, and its mean value becomes 7.0 ± 1.3 (Table 3, Fig. 3). Thus on average the observed value is only 4 % less than the one predicted for the white disk. The slope of the best-fit line through the origin for $(c + K_L)_{\mathrm{phot}}$ as a function of $1/Z_{\mathrm{D,white}}$ becomes 7.5. The deviation between the observed $(c + K_L)_{\mathrm{phot}}$ and its estimate $7.5/Z_{\mathrm{D,white}}$ obtains an rms value of $0.23\,\mathrm{m^{-1}}$, which represents 21 % of the mean value of $(c + K_L)_{\mathrm{phot}}$ (Table 3).

The agreement between $\ln(A)$ of Eq. (21) and the observed $Z_{\mathrm{D}}(c + K_L)_{\mathrm{phot}}$ that we find for the white disk is reduced when the Secchi disk is observed through coloured glass filters. In this case the observed mean values of $Z_{\mathrm{D}}(c + K_L)_{\mathrm{phot}}$ are more than 30 % smaller than the estimated mean values of $\ln(A)$ (Table 3). We speculate if there may be a spectral dependence of C_{t}.

The observed depths $Z_{\mathrm{D,black}}$ of the black disk and the related products $Z_{\mathrm{D,black}}(c + K_L)_{\mathrm{phot}}$ were also smaller than predicted. According to Table 3 the average value of

Table 9. Relationships of the forms $y = A + Bx$ and $y = B_0 x$ obtained by correlation analysis of chlorophyll *a* (Chl), total suspended material (TSM) and inverse Secchi depths ($1/Z_D$) observed with the open eye and with blue, green and red glass filters. The concentrations of Chl and TSM are averages over the depth range 0–$Z_{D,white}$, and r is the correlation coefficient. The error ε is the root mean square of the deviations ($y-A-Bx$), and ε_0 is the rms of ($y-B_0x$). The analysis is based on 41 (Chl) and 51 (TSM) stations north of 57.0° N.

y [mg m^{-3}]	x [m^{-1}]	r	A [mg m^{-3}]	B [mg m^{-2}]	B_0 [mg m^{-2}]	$(y/x)_{mean\pm sd}$ [mg m^{-2}]	$y_{mean\pm sd}$ [mg m^{-3}]	ε [mg m^{-3}]	ε_0 [mg m^{-3}]
Chl	$1/Z_{D,white}$	0.16	1.50	1.7	8.5	11.5 ± 6.2	1.8 ± 1.0	0.9	1.1
Chl	$1/Z_{D,blue}$	0.16	1.50	1.0	5.0	5.8 ± 3.1	1.8 ± 1.0	1.0	1.7
Chl	$1/Z_{D,green}$	0.09	1.71	0.3	3.0	8.0 ± 4.1	1.8 ± 1.0	0.9	1.4
Chl	$1/Z_{D,red}$	0.24	1.33	1.5	4.9	6.2 ± 3.1	1.8 ± 1.0	0.9	1.1
y [g m^{-3}]	x [m^{-1}]	r	A [g m^{-3}]	B [g m^{-2}]	B_0 [g m^{-2}]	$(y/x)_{mean\pm sd}$ [g m^{-2}]	$y_{mean\pm sd}$ [g m^{-3}]	ε [g m^{-3}]	ε_0 [g m^{-3}]
TSM	$1/Z_{D,white}$	0.76	0.12	6.2	6.8	7.1 ± 3.0	1.2 ± 0.8	0.5	0.5
TSM	$1/Z_{D,blue}$	0.54	0.71	1.4	2.5	3.6 ± 1.9	1.2 ± 0.8	0.6	0.8
TSM	$1/Z_{D,green}$	0.68	0.27	3.8	4.6	5.1 ± 2.4	1.2 ± 0.8	0.5	0.6
TSM	$1/Z_{D,red}$	0.73	0.08	3.6	3.8	4.0 ± 1.8	1.2 ± 0.8	0.5	0.5

$Z_{D,black}(c + K_L)_{phot}$ should be equal to $\ln(A) = 4.7$ for the 30 cm black disk, but the observed mean value is only 40 % of this. Observations with a black bowl, $Z_{B,black}$, resulted in 20–30 % greater depths than with the black disk, but the product $Z_{B,black}(c + K_L)_{phot}$ is still less than half of the predicted value. One explanation for the deviation could be that the black bowl is not perfectly black. It could also be that the use of colour filters and a black disk or bowl introduces effects that we have not included in $\ln(A)$.

If the diameters of the white and black disks are reduced from 30 to 10 cm, the values of C_t and W will change, and the corresponding Secchi depths including colour filter observations are predicted by the right-hand side of Eq. (21) to be reduced within the range 13–22 %. The observations show that the decrease in size reduces the Secchi depth on average by 10–20 %, in agreement with this theoretical estimate (Table 4). The best-fit line through the origin for all depths of the 10 cm disk as a function of the depths of the 30 cm disk obtains a slope of 0.83 (Fig. 4), indicating an average Secchi depth reduction of 17 % for the 10 cm disk.

The use of a telescope changes $\bar{\rho}_{L,air}$ to 0 and W to 1, and according to Eq. (21) the depth of the 30 cm white disk should then increase by 12 %. A few earlier observations confirm this estimate. Experiments made with a 10 cm disk (Table 4) show that the telescope increases $Z_{D,white,10}$ on average by 14 %, and that the effect on $Z_{D,filter,10}$ is of the same order of magnitude. If all open-eye and filter observations are put together (Fig. 5), the best-fit line through the origin obtains the slope 1.19. Thus we may state, based on Table 4, that the use of a telescope increases Z_D within the range 10–20 %.

There is practically no difference between observations of the white Secchi disk on the sunlit and shadow sides of the ship (Fig. 6), while the depths observed with colour filters may be reduced by up to 17 % on the shadow side (Table 4).

The mean value ± the standard deviation of the ratio $(c+K_L)_{phot}/(c+K_L)_{555}$ becomes 1.03 ± 0.01, supporting our assumption in Sect. 2 about the monochromatic character of the photopic coefficients. Similarly, the ratios c_{phot}/c_{555} and $c_{phot,disk}/c_{555}$ are both 1.02 ± 0.01, while the mean value and standard deviation of $K_{L,phot}/K_{L,555}$ are greater, 1.11 ± 0.05 (Table 5). The attenuation coefficients $c_{phot,filter}$ and $K_{L,filter}$ derived from luminances observed through colour filters are strongly correlated with the corresponding monochromatic coefficients with correlation coefficients very close to 1.0 (Table 5). The slope of the best-fit line through the origin for the blue and green filters obtains values between 0.95 and 1.01, while the red filter deviates more from 1.0 with the slopes 1.06 and 1.21. Thus our conclusion is that the monochromatic assumption works satisfactorily.

The correlation coefficient r is 0.95 for the linear relationship between c_{555} and $1/Z_{D,white}$, while r is reduced to 0.72 for $K_{L,555}$ as a function of $1/Z_{D,white}$ (Table 6). Similar results are found for the other MERIS channels at 412, 443, 490, 510, 620 and 665 nm. While r is in the range 0.86–0.95 for c, it is reduced to the range 0.66–0.78 for K_L. This result is reasonable since c contributes more than K_L to the sum $(c + K_L)$ which determines $Z_{D,white}$. The correlation coefficients for K_d as a function of $1/Z_{D,white}$ at the MERIS channels are in the range 0.59–0.86, and for K_u in the range 0.43–0.72 (Table 6). The errors of the estimated vertical coefficients are greatest for K_u and smallest for K_L. In the blue and green parts of the spectrum there are no significant differences between the best-fit line through the origin and the line with a constant term. At 665 nm, however, the introduction of a constant term reduces the rms error from 0.21 m^{-1} to 0.07 m^{-1} (Fig. 7).

Linear relationships between the Secchi depths observed through glass filters and the coefficients c, K_L, K_d and K_u at the wavelengths of peak visual sensitivity at 470, 540 and

Table 10. Nomenclature.

Symbol	Description	Introduced
A	Dimensionless function	Eq. (20)
A	Constant of correlation analysis	Sect. 4.5
A_1	Dimensionless function	Eq. (21)
A_2	Dimensionless function	Eq. (21)
a_{bp}	Absorption coefficient of bleached particles	Sect. 3.1
a_{y}	Absorption coefficient of yellow substance	Sect. 3.1
B	Constant of correlation analysis	Sect. 4.5
B_0	Constant of correlation analysis	Sect. 4.5
b_{p}	Scattering coefficient of particles	Sect. 3.1
C	Visual contrast between Secchi disk and background	Eq. (1)
C_{air}	Contrast of the Secchi disk observed in air	Eq. (13)
Chl	Concentration of chlorophyll a	Sect. 3.4
C_{t}	Visual threshold contrast	Eq. (1)
c	Beam attenuation coefficient	Eq. (2)
c_{phot}	Beam attenuation coefficient for nadir luminance	Sect. 4.1
D	Diameter of the Secchi disk	Eq. (14)
E_{air}	Downward illuminance or irradiance in air	Eq. (17)
E_{d}	Downward illuminance or irradiance in the sea	Eq. (6)
E_{u}	Upward illuminance or irradiance in the sea	Sect. 3.4
H	Height of the observer's eye above the surface of the sea	Eq. (22)
j	Angle of refraction in water	Eq. (22)
K_{d}	Average vertical attenuation coefficient of downward irradiance	Sect. 5.1
K_L	Average vertical attenuation coefficient of $L(z)$	Eq. (9)
$K_{L,\mathrm{phot}}$	Average vertical attenuation coefficient of luminance from nadir	Sect. 4.1
K_{q}	Average vertical attenuation coefficient of quanta irradiance (PAR)	Eq. (24)
K_{u}	Average vertical attenuation coefficient of upward irradiance	Sect. 5.1
k	$787\,\mathrm{m\,s^{-1}}$	Eq. (14)
L	Nadir radiance and luminance from the background in the sea	Eq. (1)
L_{D}	Nadir radiance and luminance from the Secchi disk	Eq. (1)
L_{r}	Radiance from sun and sky reflected at the surface	Eq. (12)
L_{w}	Water-leaving radiance	Eq. (12)
L_*	Path function along path outside the disk	Eq. (3)
$L_{*\mathrm{D}}$	Path function along path from disk to observer	Eq. (2)
n	Index of refraction for water	Eq. (12)
Q	Radiance/irradiance ratio	Sect. 3.4
R^2	Coefficient of determination	Sect. 4.4
R_L	Sub-surface radiance reflectance of the sea	Eq. (7)
r	Correlation coefficient	Sect. 4.4
$\Re$	Radiance/irradiance ratio	Eq. (18)
s_{d}	Standard deviation	Table 4
s_x	Standard deviation of x	Sect. 4.4
s_y	Standard deviation of y	Sect. 4.4
$S_{x,y}$	Covariance of x and y	Sect. 4.4
T_{D}	Transmittance of quanta irradiance between the surface and the Secchi depth	Eq. (24)
TSM	Concentration of total suspended material	Sect. 3.4
Turb	Turbidity	Sect. 5.3
U	Wind speed	Eq. (14)
W	Contrast transmittance at the water–air interface	Eq. (14)
x	Independent variable	Sect. 4.4
y	Dependent variable	Sect. 4.4
z	Vertical coordinate, positive downwards, zero at surface	Eq. (2)
$Z_{\mathrm{B,black}}$	Secchi depth of the black bowl	Sect. 4.5
$Z_{\mathrm{D,black}}$	Secchi depth of the black disk	Sect. 4.5
$Z_{\mathrm{D,blue}}$	Secchi depth of the white disk observed with blue filter	Sect. 4.5
$Z_{\mathrm{D,green}}$	Secchi depth of the white disk observed with green filter	Sect. 4.5
$Z_{\mathrm{D,red}}$	Secchi depth of the white disk observed with red filter	Sect. 4.5
$Z_{\mathrm{D,white}}$	Secchi depth of the white disk observed with naked eye	Eq. (5)
$Z_{\mathrm{q}}(p\,\%)$	Depth where the quanta irradiance is reduced to p % of the surface value	Sect. 5.2
α	Apparent angle from the observer's eye across the Secchi disk	Eq. (22)
ε	Root-mean-square error	Sect. 4.8
ε_0	Root-mean-square error	Sect. 4.8
λ	Wavelength	Sect. 3.1
ρ_{DL}	Luminance or radiance reflectance of the Secchi disk	Eq. (6)
$\bar{\rho}_{L,\mathrm{air}}$	Fresnel-reflected luminance or radiance towards the zenith	Eq. (17)
τ	Luminance or radiance transmittance for a ray of normal incidence at the water–air interface	Eq. (12)

620 nm (Table 2) have also been calculated (Table 7). The rms errors of the estimated coefficients are in the range 0.07–0.47 m^{-1}, or 10–80 % of the corresponding mean values. The accuracy of the estimates based on the white disk and naked eye is equal to or better than the estimates from colour filter observations.

The mean vertical attenuation coefficient of quanta irradiance or PAR between the surface and the Secchi depth, K_q, may be estimated from $1/Z_{D,white}$ with an rms error less than 22 % of the mean value of K_q (Table 8). The mean values of the ratios $Z_q(10\,\%)/Z_{D,white}$ and $Z_q(1\,\%)/Z_{D,white}$ are 0.9 and 2.2, respectively, or very close to 1 and 2. Table 8 shows that estimates of Z_q from observed $Z_{D,white}$ will have relative errors in the range 20–30 %. The depth of the euphotic zone may be defined as $Z_q(1\,\%)$ (Fig. 8), and according to Table 8 this depth can be estimated by an rms error of 24 %. Consequently these relationships will provide very useful checks of our irradiance measurements. Relationships for $Z_q(3\,\%)$, $Z_q(10\,\%)$ and $Z_q(30\,\%)$ as functions of $Z_q(1\,\%)$ are presented in Fig. 9 and Table 8.

The Secchi depth may also be used to estimate the concentrations of chlorophyll *a* (Chl) and total suspended material (TSM) (Fig. 10). The estimates of Chl and TSM as functions of $1/Z_D$ have average errors of 50–90 % and 40–70 %, respectively (Table 9, Fig. 10). Still, these estimates will provide the order of magnitude of the concentrations.

Our overall conclusion becomes that Eq. (21) quantifies well the relationships between the white disk and the optical attenuation coefficients, but less so for the colour filters and the black disk. The Secchi depths provide very useful checks of the monochromatic attenuation coefficients and of chlorophyll *a* and total suspended material. We assume that there may be regional differences for the found relationships, and they should be tested out for different oceanic regions and water types.

Acknowledgements. The in-water spectral irradiance and radiance data from the Oslofjord–Skagerrak area were collected in 2002–2003, as parts of two validation projects: "Validation of MERIS Data Products" (VAMP) funded by ESA, the Norwegian Space Centre and the Norwegian Institute for Water Research (PRODEX contract no. 14849/00/NL/Sfe(IC)), and "Regional Validation of MERIS Chlorophyll Products in North Sea Coastal Waters" (REVAMP), funded by an FP5 research contract from the European Commission (contract no. EVG1–CT–2001–00049).

Edited by: M. Hoppema

References

Aarup, T.: Transparency of the North Sea and Baltic Sea – a Secchi depth data mining study, Oceanologia, 44, 323–337, 2002.

Aarup, T., Holt, N., and Højerslev, N. K.:, Optical measurements in the North Sea-Baltic Sea transition zone, II. Water mass classification along the Jutland west coast from salinity and spectral irradiance measurements, Cont. Shelf Res., 16, 1343–1353, 1996a.

Aarup, T., Holt, N., and Højerslev, N. K.: Optical measurements in the North Sea-Baltic Sea transition zone, III. Statistical analysis of bio-optical data from the Eastern North Sea, the Skagerrak and the Kattegat, Cont. Shelf Res., 16, 1355–1377, 1996b.

Aas, E.: Estimates of radiance reflected towards the zenith at the surface of the sea, Ocean Sci., 6, 861–876, doi:10.5194/os-6-861-2010, 2010.

Aas, E. and Højerslev, N. K.: Analysis of underwater radiance observations: Apparent optical properties and analytic functions describing the angular radiance distribution. J. Geophys. Res., 104, 8015–8024, 1999.

Aas, E. and Høkedal, J.: Reflection of spectral sky irradiance on the surface of the sea and related properties, Remote Sens. Environ., 70, 181–190, 1999.

Aas, E. and Korsbø, B.: Self-shading effect by radiance meters on upward radiance observed in coastal waters, Limnol. Oceanogr., 42, 968–974, 1997.

Aas, E., Andresen, T., Løyning, T., and Sørgård, E.: Eutrofisituasjonen i Ytre Oslofjord. Delprosjekt 3.7: Optiske observasjoner – Overflatevannets kvalitet sett ut fra observasjoner i overflatelaget. SFT (Norw. Environ. Agency) Report 388/90, 50 pp., 1989.

Aas, E., Højerslev, N. K., and Høkedal, J.: Conversion of subsurface reflectances to above-surface MERIS reflectance, Int. J. Remote Sens., 30, 5767–5791, 2009.

Andresen, A.: Siktedyputviklingen i Oslofjorden 1936–92, Master thesis, Dept. Geophys., Univ. Oslo, 228 pp., 1993.

Aure, J., Molvær, J., and Stigebrandt, A.: Observations of inshore water exchange forced by a fluctuating offshore density field, Mar. Poll. Bull., 33, 112–119, 1996.

Blackwell, H. R.: Contrast thresholds of the human eye, J. Opt. Soc. Am., 36, 624–632, 1946.

Boguslawski, G. V.: Handbuch der Ozeanographie, Band I. Räumliche, physikalische und chemische Beschaffenheit der Ozeane, Verlag von J. Engelhorn, Stuttgart, 400 pp., 1884.

Cox, C. and Munk, W.: Statistics of the sea surface derived from sun glitter, J. Mar. Res., 13, 198–227, 1954a.

Cox, C. and Munk, W.: The measurements of the roughness of the sea surface from photographs of the sun's glitter, J. Opt. Soc. Am., 44, 838–850, 1954b.

Davies-Colley, R. J.: Measuring water clarity with a black disc, Limnol. Oceanogr., 33, 616–623, 1988.

Duntley, S. Q.: The visibility of submerged objects. Final Rep., Visibility Lab., Mass. Inst. Tech., 74 pp., 1952.

Fleming-Lehtinen, V. and Laamanen, M.: Long-term changes in Secchi depth and the role of phytoplankton in explaining light attenuation in the Baltic Sea, Est. Coast. Shelf Sci., 102–103, 1–10, 2012.

Gade, H. G.: Some hydrographic observations of the Inner Oslofjord during 1959, Hvalrådets skrifter, Nr. 46, Universitetsforlaget, Oslo, 62 pp., 1963.

Gade, H. G.: Delrapport nr. 2, Hydrografi. Oslofjorden og dens forurensningsproblemer, I. Undersøkelsen 1962–1965, Norsk institutt for vannforskning, Oslo, 164 pp., 1967.

Gordon, H. R. and Ding, K.: Self-shading of in-water optical instruments. Limnol. Oceanogr., 37, 491–500, 1992.

Gordon, H. R. and Wouters, A. W.: Some relationships between Secchi depth and inherent optical properties of natural waters, Appl. Opt., 17, 3341–3343, 1978.

Gröen, P. and Dorrestein, R.: Zeegolven. KNMI Opstellen op Oceanografisch en Maritiem Meteorologisch Gebied, 11, 124 pp., 1976.

Haltrin, V. I.: Spectral relative clarity of Black and Aegan Seas. Geoscience and Remote Sens. Symp. Proc., IGARSS '98. 1998 IEEE International, 2, 913–915, 1998.

Holmes, R. W.: The Secchi disk in turbid coastal waters, Limnol. Oceanogr., 15, 688–694, 1970.

Hou, W., Lee, Z., and Weidemann, A. D.: Why does the Secchi disk disappear? An imaging perspective, Optics Expr., 15, 2791–2802, 2007.

Højerslev, N. K.: Spectral daylight irradiance and light transmittance in natural waters measured by means of a Secchi Disc only, Int. Council Explor. Sea, C. M. 1977/C:42, 19 pp., 1977.

Højerslev, N. K.: Daylight measurements appropriate for photosynthetic studies in natural sea waters, J. Cons. Int. Explor. Mer., 38, 131–146, 1978.

Højerslev, N. K.: Bio-optical measurements in the Southwest Florida Shelf ecosystem, J. Cons. Int. Explor. Mer, 42, 65–82, 1985.

Højerslev, N. K.: Visibility of the sea with special reference to the Secchi disc, Ocean Optics VIII, SPIE Vol. 637, 294–305, 1986.

Højerslev, N. K., Holt, N., and Aarup, T.: Optical measurements in the North Sea-Baltic Sea transition zone, I. On the origin of the deep water in the Kattegat, Cont. Shelf Res., 16, 1329–1342, 1996.

Høkedal, J. and Aas, E.: Observations of spectral sky radiance and solar irradiance. Rep. 103, Dept. Geophys., Univ. Oslo, Oslo, 73 pp., 1998.

Ibrekk, H. O. and Holtan, G.: Eutrofisituasjonen i Ytre Oslofjord, Delprosjekt 3.1: Forurensningstilførsler til Ytre Oslofjord, NIVA-Rapport 352/88, Oslo, 44 pp., 1988.

Jerlov, N. G.: Marine Optics. Elsevier, Amsterdam, 231 pp., 1976.

Kratzer, S., Håkansson, B., and Sahlin, C.: Assessing Secchi and photic zone depth in the Baltic Sea from satellite data, Ambio, 32, 577–585, 2003.

Krümmel, O.: Der Ozean, Eine Einführung in die allgemeine Meereskunde, G. Freytag, Leipzig, F. Tempsky, Prag, 242 pp., 1886.

Krümmel, O.: Bemerkungen über die Durchsichtigkeit des Meerwassers, Ann. d. Hydr. mar. Met., 2, 62–78, 1889.

Krümmel, O.: Handbuch der Ozeanographie, Band I. Die räumlichen, chemischen und physikalischen Verhältnisse des Meeres, Verlag von J. Engelhorn, Stuttgart, 526 pp., 1907.

Levin, I. M.: Theory of the white disk, Izvest. Atmos. Ocean. Phys., 16, 678–683, 1980.

Lisitzin, E.: Über die Durchsichtigkeit des Wassers im nördlichen Teil des Baltischen Meeres, Fennia, 65, 1–22, 1938.

Mikaelsen, B. and Aas, E.: Secchi disk depths and related quantities in the Oslofjord 1986–87, Rep. 77, Dept. Geophys., Univ. Oslo, Oslo, 55 pp., 1990.

Mobley, C. D.: Estimation of the remote-sensing reflectance from above-surface measurements, Appl. Opt., 38, 7442–7455, 1999.

Morel, A. and Gentili, B.: Diffuse reflection of oceanic waters, III. Implication of bi-directionality for the remote-sensing problem, Appl. Opt., 35, 4850–4862, 1996.

Morel, A., Huot, Y., Gentili, B., Werdell, P. J., Hooker, S. B., and Franz, B. A., Examining the consistency of products derived in open ocean (Case 1) waters in the perspective of a multi-sensor approach. Remote Sens. Environ., 111, 69–88, 2007.

Paulson, C. A. and Simpson, J. J.: Irradiance measurements in the upper ocean, J. Phys. Oceanogr., 7, 952–956, 1977.

Preisendorfer, R. W.: Secchi disk science: Visual optics of natural waters, Limnol. Oceanogr., 31, 909–926, 1986.

Sandén, P. and Håkansson, B.: Long-term trends in Secchi depth in the Baltic Sea, Limnol. Oceanogr., 41, 346–351, 1996.

Sauberer, F. and Ruttner, F.: Die Strahlungsverhältnisse der Binnengewässer, Akademische Verlagsgesellschaft, Leipzig, 240 pp., 1941.

Secchi, A.: Esperimente per determinare la transparenza del mare, in: Sul moto ondoso del mare e su le correnti di esso specialmente su quelle littorali, edited by: Cialdi, A., Rome, 258–288, 1866.

Shifrin, K. S.: Physical optics of ocean water, Am. Inst. Phys., New York, 285 pp., 1988.

Staalstrøm, A., Aas, E., and Liljebladh, B.: Propagation and dissipation of internal tides in the Oslofjord, Ocean Sci., 8, 525–543, doi:10.5194/os-8-525-2012, 2012.

Sørensen, K. and Aas, E.: Remote sensing of water quality, Proc. SPIE vol. 2258, Ocean Optics XII, edited by: Jaffe, J. S., 332–341, 1994.

Sørensen, K., Aas, E., Faafeng, B., and Lindell, T.: Fjernmåling av vannkvalitet – Videreutvikling av optisk satellittfjernmåling som metode for overvåking av vannkvalitet, NIVA Rep., ISBN 82-577-2262-6, 115 pp., 1993.

Sørensen, K., Høkedal, J., Aas, E., Doerffer, R., and Dahl, E.: Early results for validation of MERIS water products in the Skagerrak. Proceedings of Envisat Validation Workshop, 9–13 December 2002, Frascati, Italy, ESA SP-531, March 2003, 2003.

Sørensen, K., Aas, E., Høkedal, J., Severinsen, G., Doerffer, R., and Dahl, E.: Validation of MERIS water products in the Skagerrak. MAVT Workshop. Proceedings of Envisat Validation Workshop, 20–24 October 2003, Frascati, Italy, ESA CD-ROM, 2004.

Sørensen, K., Aas, E., and Høkedal, J.: Validation of MERIS water products and bio-optical relationships in the Skagerrak, Int. J. Remote Sens., 28, 555–568, 2007.

Takenouti, Y.: On the transparency of sea water, Oceanogr. Mag., Tokyo, 4, 129–135, 1950.

Tyler, J. E.: The Secchi Disc, Limnol. Oceanogr., 13, 1–6, 1968.

Walsh, J. W.: Photometry. Dover, New York, 544 pp., 1958.

Wernand, M. R.: On the history of the Secchi disk, J. Eur. Opt. Soc., Rap. Publ., 5, 100135-1-6, 2010.

WMO: Guide to wave analysis and forecasting, 2nd Edn., WMO-No. 702, 159 pp., 1998.

Zhang, Y., Pulliainen, J., Koponen, S., and Hallikainen, M.: Empirical algorithms for Secchi disk depth using optical and microwave remote sensing data from the Gulf of Finland and the Archipelago Sea, Boreal Environ. Res., 8, 251–261 (ISSN 1239-6095), 2003.

Zibordi, G. and Ferrari, G. M.: Instrument self-shading in underwater optical measurements: experimental data, Appl. Opt., 34, 2750–2754, 1995.